

March 2018

Design of Micro-Scale Energy Harvesting Systems for Low Power Applications Using Enhanced Power Management System

Majdi M. Ababneh

University of South Florida, mababneh@mail.usf.edu

Follow this and additional works at: <http://scholarcommons.usf.edu/etd>

 Part of the [Electrical and Computer Engineering Commons](#)

Scholar Commons Citation

Ababneh, Majdi M., "Design of Micro-Scale Energy Harvesting Systems for Low Power Applications Using Enhanced Power Management System" (2018). *Graduate Theses and Dissertations*.
<http://scholarcommons.usf.edu/etd/7117>

This Dissertation is brought to you for free and open access by the Graduate School at Scholar Commons. It has been accepted for inclusion in Graduate Theses and Dissertations by an authorized administrator of Scholar Commons. For more information, please contact scholarcommons@usf.edu.

Design of Micro-Scale Energy Harvesting Systems for Low Power Applications Using Enhanced
Power Management System

by

Majdi Mohammad Khair Ababneh

A dissertation submitted in partial fulfillment
of the requirements for the degree of
Doctor of Philosophy
Department of Electrical Engineering
College of Engineering
University of South Florida

Major Professor: Sylvia Thomas, Ph.D.
Frank Pyrtle, Ph.D.
Henry Cabra, Ph.D.
Ismail Uysal, Ph.D.
Nasir Ghani, Ph.D.

Date of Approval:
February 28, 2018

Keywords: power efficiency, mini notched turbine, MPPT, RF rectenna,
DC-DC converter, resistor emulation, PSO

Copyright © 2018, Majdi Mohammad Khair Ababneh

DEDICATION

This dissertation is dedicated to my father Mohammad Khair Ababneh for being the perfect father, for his support, inspiration, and for sacrificing all his life for us, our family and country; to my mother Helda Ababneh for her encouragement, continuous prayers. To my lovely sisters: Elham and Maysoon; and my brothers: Mustafa, Ahmad, Mahmoud, and Hamzeh.

ACKNOWLEDGMENTS

This dissertation was possible because I could collaborate with the research team of the AMBIR (Advance Materials Bio and Integration Research Laboratory) group. It was gratifying and was an absolute privilege to have Professor Sylvia W Thomas as an adviser, who taught me research is a story to be presented to the world so that mankind can benefit, and the world becomes greener and a better place to live in because of my work.

I'm sincerely thankful to Prof. Frank Pyrtle, Prof. Henry Cabra, Prof. Ismail Uysal, and Prof. Nasir Ghani for their acceptance to join the presentation of my defense and spending their valuable time to read my dissertation. Also, I'm sincerely thankful to Prof. Tan Yen Kheng for his help and support.

I am very grateful to the administration, faculty, and staff of the University of South Florida, the college of engineering, the electrical engineering department, AMBIR lab, and the WAMI center for supporting the diversity, providing employment opportunities for the international student, and offering a great environment for working and studying. I'm also very grateful to Prof. Selcuk Kose for his help and support during my Ph.D; he greatly helped me to join USF.

In my research laboratory here in USF, I am really fortunate to be surrounded by a bunch of good and friendly people, who are always there to help me. These people, whom are all my past and present lab-mates, include Samuel Perez, William Serrano, Manopriya Devisetty, Kavyashree Puttananjegowda, Ridita Khan, and Nirmita Roy, and so on. I must express a big

thank you to all of you for spending their valuable time in all possible discussions and their precious company and help. I have really spent an enjoyable and memorable life with them during my stay at USF.

For their help and support at USF, I would like to thank to my friends, Derar Hawatmeh, Mohammad Jasim, Orhun Uzun, Ahmad Gheethaan, Abdulla Qaroot, Fayik Alrabee, Amar Amouri, Mohammad Mounir, Mohammad Kurdi, Mohammad Hafez, Asim Mazin, and Sai Bharadwaj and Andrew Escobar.

I also would like to offer special exceptional thanks to Aidas Nasevicius, Julie Nasevicius, and Anne Leske, who have helped and supported me throughout this process.

I also would like to offer special thanks to Qutaiba Al-hazaim, Anas Sayaheen, Bashar Alwedyan, Khair Alshamileh, Bashar Alwedyan, Mohammad Ghraibeh, Yousef Mashaale, Hassan Diabat, Mohammad Bani Hani, Adham Otoom, Malek Khedirat, Ali Bani Amer, Mohammad Ababneh, Ali Ababneh, and all my friends from Jordan who have supported me throughout this process.

I want to thank all of my professors for their efforts through my undergraduate and graduate years. Many thanks to Prof. Mohammad Al-Salameh, Prof. Nihad for their help and support during my Master degree. I'm really thankful to them and I can't find the words to express my appreciation toward them.

My family has been supportive and patient through my years of study. I want to thank every member of my family especially my parents, sisters, and brothers. I'm also grateful and thankful to my friends in Tampa Dr. Ibrahim Nassar, Yasser Abukhait, and Amr Khrais who greatly helped me especially in my first days here in the US.

Most importantly, I'm thankful to Allah for his blessing that helped me in my achievements and reconciling me to the right way which guide me to this research.

TABLE OF CONTENTS

LIST OF TABLES	iii
LIST OF FIGURES	iv
ABSTRACT	vii
CHAPTER 1: INTRODUCTION	1
1.1 Energy Harvesting System	2
1.1.1 Energy Harvesting Source	2
1.1.2 Power Management Circuit	3
1.2 Objectives	4
1.3 Organization	4
CHAPTER 2: ENERGY HARVESTING SYSTEM	7
2.1 Introduction	7
2.2 Background	8
2.3 Mini Notched Turbine Energy Harvesting Source	9
2.3.1 Mini Notched Turbine Energy Harvesting Source	10
2.3.1.1 CAD Design	12
2.3.1.2 Rotor Design	12
2.3.1.3 Overall System	13
2.4 Mini Notched Turbine Generator	14
2.5 RF Energy Harvesting Source (Rectenna)	20
2.5.1 Introduction	21
2.5.2 Background	21
2.5.3 RF Rectenna	22
2.5.3.1 Antenna Design	25
2.5.3.2 Matching Network	25
2.5.3.3 Rectifier Circuit	27
2.5.4 Fabricated RF Rectenna	28

CHAPTER 3: OVERVIEW OF POWER MANAGEMENT CIRCUITS	32
3.1 Introduction	32
3.2 Maximum Power Point Tracking System	33
3.2.1 Resistor Emulation Technique Using DC-DC Converter	35
3.2.2 Overview of Boost DC-DC Converter	36
3.2.2.1 The Discontinuous Conduction Mode	38
3.3 MPPT with Resistor Emulation Technique Using Boost DC-DC Converter	40
3.3.1 Power Loss Analysis	41
3.3.2 Control Circuit	43
3.4 Boost Converter Configuration with PSO Technique	45
3.4.1 Particle Swarm Optimization (PSO) Technique	45
3.4.1.1 PSO Language for MPPT	47
3.4.1.2 PSO Flow Chart	48
3.4.1.3 Velocity and Position Updates	49
3.4.2 PSO Parameters Value Selection	50
3.4.3 Selection of L and D_1T_s	50
3.5 Simulation Results	51
 CHAPTER 4: IMPLEMENTATION OF ENERGY HARVESTING SYSTEM WITH ENHANCED MAXIMUM POWER TRACKING SYSTEM USING DC-DC BOOST CONVERTER AND RESISTOR EMULATION	 56
4.1 Introduction	56
4.2 Architecture of the Implemented Energy Harvesting System Design	57
4.3 Mini Notched Energy Harvesting System	57
4.3.1 Enhanced Power Management Circuit Using DC-DC Converter	60
4.3.2 Experimental Results	62
4.4 RF Rectenna Energy Harvesting System	68
4.4.1 Experimental Results	68
4.5 Mini Notched Turbine Vs. RF Rectenna	72
 CHAPTER 5: CONCLUSIONS AND FUTURE WORK	 73
5.1 Future Work	76
 REFERENCES	 77
 APPENDICES	 88
Appendix A: Data of Figures 4.6, 4.7, 4.11, and 4.12	89
Appendix B: Copyright Notices	93
Appendix C: Glossary of Terms	97
 ABOUT THE AUTHOR	 End Page

LIST OF TABLES

Table 1.1	Energy Harvesting Sources with Their Power/Energy Densities.	2
Table 2.1	State of the Art of Energy Harvesting Sources [1, 5, and 8-15].	10
Table 2.2	Comparison of Conversion Efficiency in Different Configurations of Rectenna [59].	26
Table 2.3	Commercial Schottky Diodes.	29
Table 3.1	PSO Parameters.	50
Table 3.2	PSO Parameters Values Used in Optimization.	53
Table 4.1	Enhanced Power Management Circuit Parameters.	64
Table A.1	Power Conversion Efficiency of Enhanced Power Management Circuit for Low Input Power Range Using MiNT.	89
Table A.2	Power Conversion Efficiency of Enhanced Power Management Circuit for High Input Power Range Using MiNT.	90
Table A.3	Power Conversion Efficiency of Enhanced Power Management Circuit for Low Input Power Range Using RF Rectenna.	91
Table A.4	Power Conversion Efficiency of Enhanced Power Management Circuit for High Input Power Range Using RF Rectenna.	92

LIST OF FIGURES

Figure 1.1	Basic components of an energy harvesting system.	3
Figure 1.2	Renewable energy sources.	4
Figure 2.1	Overview of energy harvesting system [23, 24].	11
Figure 2.2	Block diagram illustrating proposed integrated mini notched [12].	12
Figure 2.3	Mini notched turbine design [11, 12].	14
Figure 2.4	Different mini notched turbine approaches with volumetric size of; a) $27*27*6 \text{ mm}^3$, b) $41.8*41.8*14.1 \text{ mm}^3$, c) $41*41*8.5 \text{ mm}^3$, and d) $46.8*43.8*12.4 \text{ mm}^3$ [12].	16
Figure 2.5	Nozzle velocity simulation [11, 12].	17
Figure 2.6	Block diagram of mini notched turbine [11, 12].	17
Figure 2.7	Power curves of MiNT generator over a range of flow speeds and different resistance loadings.	19
Figure 2.8	Measured generated power against output voltage for two MiNT approaches [19, 36].	20
Figure 2.9	Measured I-V characteristics of mini notched turbine for different flow speeds [19, 36].	20
Figure 2.10	Block diagram of RF energy harvesting system.	23
Figure 2.11	Matching network techniques.	28
Figure 2.12	Equivalent circuit model of Schottky diode.	29
Figure 2.13	Fabricated rectenna with matching network and rectifier stage.	30
Figure 2.14	Simulation results of power generated by rectenna over a range of input power for different loads.	30

Figure 2.15	Measurement and simulation results for the efficiency of rectenna.	31
Figure 3.1	Energy harvesting system using DC-DC converter as matching impedance.	34
Figure 3.2	Boost DC-DC converter configuration.	37
Figure 3.3	Boost DC-DC converter circuit when the MOSFET is on.	37
Figure 3.4	Boost DC-DC converter circuit when the MOSFET is off.	38
Figure 3.5	The waveform of inductor current.	39
Figure 3.6	Maximum power point tracking system using boost DC-DC converter.	41
Figure 3.7	MPPT design using programmable oscillator and comparator.	45
Figure 3.8	Flow chart of PSO presenting MPPT configurations.	52
Figure 3.9	Simulation at different values of R_{em} (50-800 Ω) over P_{in} range (50 μ W-500 μ W).	54
Figure 3.10	PSO simulation results vs. simulation results of passive MPPT [38, 39] of converter efficiency for R_{em} (200 and 750 Ω) and simulation results of adaptive MPPT [24] for $R_{em} = 1000 \Omega$.	54
Figure 3.11	Power loss calculations of a DC-DC converter for input power range of (0.15-5mW).	55
Figure 4.1	Architecture of energy harvesting system design.	58
Figure 4.2	Circuit configuration of energy harvesting system using MiNT [12].	59
Figure 4.3	Proposed enhanced MPPT.	61
Figure 4.4	Energy harvesting system; a) Enhanced power management system and b) Mini notched turbine [12].	62
Figure 4.5	The test configuration to measure mini notched turbine energy harvesting performances [12].	63
Figure 4.6	Power conversion efficiency of DC-DC boost converter with proposed resistor emulation technique for low input power range.	65
Figure 4.7	Power conversion efficiency of DC-DC boost converter with proposed resistor emulation technique for mild input power range.	66

Figure 4.8	Power conversion efficiency comparison in a DC-DC converter over (200 μ -1mW) power input range between the enhanced MPPT and MPPT in [24] and [38, 39].	67
Figure 4.9	Power conversion efficiency comparison in a DC-DC converter over (1mW-10mW) power input range between the enhanced MPPT and MPPT in [23] and [35].	67
Figure 4.10	RF rectenna energy harvesting system with enhanced MPPT.	69
Figure 4.11	Power conversion efficiency of DC-DC boost converter with proposed resistor emulation technique for low input power range coming from RF rectenna.	70
Figure 4.12	Power conversion efficiency of DC-DC boost converter with proposed resistor emulation technique for input power range coming from RF rectenna.	71

ABSTRACT

The great innovations of the last century have ushered continuous progress in many areas of technology, especially in the form of miniaturization of electronic circuits. This progress shows a trend towards consistent decreases in power requirements due to miniaturization. According to the ITRS and industry leaders, such as Intel, the challenge of managing and providing power efficiency still persist as scaling down of devices continues. A variety of power sources can be used in order to provide power to low power applications. Few of these sources have favorable characteristics and can be designed to deliver maximum power such as the novel mini notched turbine used as a source in this work. The MiNT is a novel device that can be used as a feasible energy source when integrated into a system and evaluated for power delivery as investigated in this work. As part of this system, a maximum power point tracking system provides an applicable solution for capturing enhanced power delivery for an energy harvesting system. However, power efficiency and physical size are adversely affected by the characteristics and environment of many energy harvesting systems and must also be addressed. To address these issues, an analysis of mini notched turbine, a RF rectenna, and an enhanced maximum power point tracking system is presented and verified using simulations and measurements. Furthermore, mini notched energy harvesting system, RF rectenna energy harvesting system, and enhanced maximum power point tracking system are developed and experimental data analyzed. The enhanced maximum power point tracking system uses a resistor emulation technique and particle swarm optimization (PSO) to improve the power efficiency and reduce the physical size.

This new innovative design improves the efficiency of optimized power management circuitry up to 7% compared to conventional power management circuits over a wide range of input power and range of emulated resistances, allowing more power to be harvested from small energy harvesting sources and delivering it to the load such as smart sensors. In addition, this is the first IC design to be implemented and tested for the patented mini notched turbine (MiNT) energy harvesting device.

Another advantage of the enhanced power management system designed in this work is that the proposed approach can be utilized for extremely small energy sources and because of that the proposed work is valid for low emulated resistances. and systems with low load resistance Overall, through the successful completion of this work, various energy harvesting systems can have the ability to provide enhanced power management as the IC industry continues to progress toward miniaturization of devices and systems.

CHAPTER 1:

INTRODUCTION

Energy harvesting is a mechanism that catches and harvests of small amounts of available energy in the environment and then converts into usable electrical energy. This electrical energy can be used directly or stored for later use. This process expands the utilizations of an energy source in locations where there is no grid power. Excluding outdoor solar, no small energy sources can produce a large amount of energy. However, the energy harvested is sufficient for most wireless applications, RFID, body implants, and remote sensing. Also, most energy harvesting sources can still be used to extend the battery life even if the gathered energy is low. The battery is the main power source for most low power devices, such as sensors, medical devices, and portable devices. However, most of batteries have a limited lifetime and must be replaced every 5-10 years [1-4]. On the other hand, Energy harvesting eliminates the needs to change the batteries and could provide continuous and sustainable power for low power devices. Most energy harvesting systems are designed to be independent, reliable, small size, and cost-effective. The development of energy harvesting technologies has been directed to explore the capability of energy harvesting sources that could harvest energy from the ambient environment. In the same time, it drives the trend for more applications such as remote sensing, submerged, portable devices, and In-vivo applications where conventional power sources are not realistic. Table 1.1 lists the state of the art in energy harvesting sources and their power/energy densities [5].

Table 1.1: Energy Harvesting Sources with Their Power/Energy Densities [5].

Energy Source	Power/Energy density	Comments
Solar cell/ambient light	100 μ -100mW/cm ²	15-30% efficiency
Thermal	30-50 μ W/ 60-150 μ W/cm ²	Low power
Wireless radio frequency	150 mW	Near a RF transmitter
Kinetic: Blood pressure fluctuations	2.4 μ W	Low power
Wind	1 mW/ cm ²	Average speed
Wireless energy transfer	14 mW/ cm ²	Short distances
Ultrasonic	21.4 nW	Low power
Kinetic Foot pressure (Piezo)	1 W	High power

1.1 Energy Harvesting System

The process of energy harvesting depends on the power source, available power, load, and application. Any energy harvesting system includes an energy source such as wind, heat, hydroelectric, light, pressure, or vibration, power management circuit system, and load as shown in Fig.1.1.

1.1.1 Energy Harvesting Source

There are many of energy sources that are not exploited. These energy sources are available in the environment and it is not necessary to overwork to extract the energy from them such as wind, solar, hydroelectric, and thermal compared to non-renewable energy sources such as oil, gas, and fossil fuels as shown in Fig. 1.2. Unlike Oil and fuel which are limited and expected to end by 2050, the majority of the renewable energy sources are sustainable for almost unlimited time.

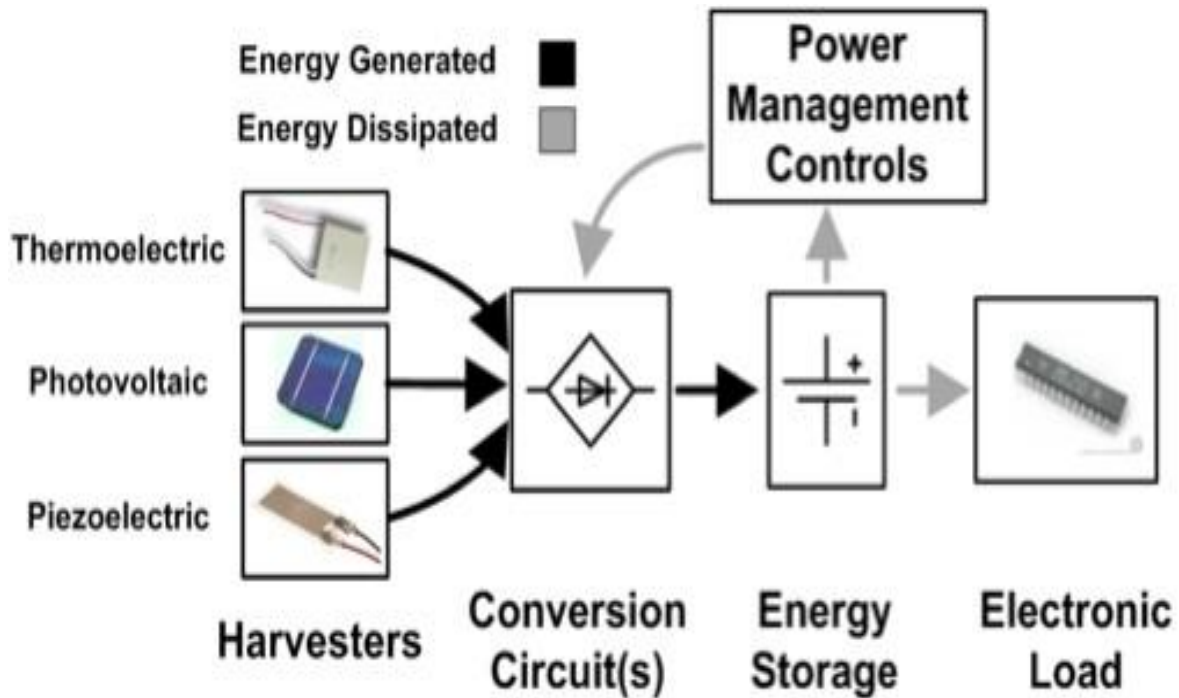


Figure 1.1: Basic components of an energy harvesting system [1].

1.1.2 Power Management Circuit

In order to harvest power from common energy sources such as turbines, thermoelectric generators, wind, and solar cells, every energy harvesting system requires power management circuit to efficiently convert, collect, store, and manage the energy from these sources into usable electrical energy for low power devices/circuits. Power Management technique is useful because it could improve the power efficiency and then eliminates the needs to change batteries. Also, could provide continuous and sustainable power for low power devices. Matching network is needed between the energy source and the electrical load to achieve maximum power delivered to the load and minimum power loss. Appropriate power management circuits for load impedance matching and power control are available commercially in Texas instruments and linear technology.



Figure 1.2: Renewable energy sources.

1.2 Objectives

This research aims to leverage the capabilities of manufacturing technique to develop power efficient energy harvesting systems that meet the requirement of today's accelerating power systems in various applications (such as medical devices, automotive, smart sensors, Internet of Things), where the power sources and power management circuits can be integrated into the system, through developing enhanced devices that are compatible with such systems. Also, it aims to explore energy harvesting system limitation/disadvantages and looking into innovative solutions to address, as well overcome these drawbacks. The developed energy harvesting systems should be proven using simulations and theories and then implemented and fabricated to validate the design.

1.3 Organization

This work is organized as follows. In Chapter 2 the mini notched turbine is introduced. It is a novel mini notched turbine that can be used as feasible energy source to meet the power

requirements of small embedded systems is presented with an overall volume smaller than 15 mm³. The Mini notched turbine consists of two parts, the turbine casing and the rotor. Mini notched turbine is being prototyped and tested on a miniaturized energy generator system, which could be used as a green energy source that converts biomechanical energy from some kinds of microfluidics to electrical energy. The Mini notched turbine has increased efficiency over traditional turbine systems due to changes in the inclination angle of the nozzle, large hub diameter and blade attachment configuration that reduces vortices and increases internal pressure. Also, A RF rectenna that can be used as feasible energy source to meet the power requirements of small embedded systems is presented in Chapter 2. RF rectenna is being prototyped and tested on a miniaturized energy generator system, which could be used as a green energy source using a matching network to ensure maximum power transfer and rectifier to convert the energy in useful DC power to use it later for low power devices. The conversion efficiency of RF rectenna is 70% for load resistance equal to 400Ω compared to 75% in simulation results.

Chapter 3 presents an approach for gathering near maximum power by improving the efficiency of DC-DC converter. Convenient power management circuits are not suitable for very low power energy sources due to the high power consumption of components that used in the system. Based on that, particle swarm optimization (PSO) technique is successfully applied to select proper values of inductor and on-time to minimize power consumption, improve DC-DC converter efficiency, and the efficiency of power management system where the converter efficiency is used as fitness function and inductor and on-time are chosen as optimized parameters. Based on this analysis the power management circuit is designed and fabricated.

In Chapter 4 the design process and the implementation of a mini notched turbine system and RF rectenna system with enhanced power management is discussed and tested.

In Chapter 5 concludes the thesis, and suggests possible future work.

CHAPTER 2:

ENERGY HARVESTING SYSTEM

2.1 Introduction

In this chapter, a novel mini notched turbine that can be used as a feasible energy source to meet the power requirements of small embedded systems is presented. A novel mini notched turbine harvester is introduced with an overall volume smaller than 15 mm^3 . The Mini notched turbine consists of two parts, the turbine casing and the rotor. Mini notched turbine is being prototyped and tested on a miniaturized energy generator system, which could be used as a green energy source that converts biomechanical energy from some kinds of microfluidics to electrical energy. The design of this novel turbine is developed with environmental and biomedical applications in mind [6-8]. Materials, size, and the assembling of parts are critical issues in design and final assembly of prototypes. In addition, bio-systems could be developed, if the system is built with biocompatible materials, transforming it into a bio micro turbine with the possibility to be used in medical devices as part of a system implanted on a living organism.

The remainder of this chapter 2 is arranged as follows. The related background and motivation for the proposed mini notched turbine is provided in Section 2.2, the characterization, analysis, and modeling of mini notched turbine is presented in Section 2.3, prototype and modeling of mini notched turbine and its measurement results are presented in Section 2.4, the characterization, analysis, and modeling of RF rectenna is discussed in Section 2.5.

2.2 Background

The great innovations of the last century have ushered continuous progress in many areas of technology, especially in the form of miniaturization of electronic circuits. This progress shows a trend towards consistent increases in memory density, processing speed and power density; and towards a decrease in power requirements due to miniaturization. It is worth noting that of all these, power density has seen the least improvement [7]. It is not surprising that many efforts are being made to rectify such disparity, since lower cost has given rise to the proliferation of portable electronic devices that need some form of power to operate. Usually, the supply of this power is in the form of rechargeable batteries and power conditioning circuits that work very well together to supply the demands for power. Although this is a good solution for extracorporeal (outside the body) devices, it is not the optimal solution for a group of portable devices. This research will make it possible to integrate a power source that converts mechanical energy to electrical energy and uses that energy to supply most medical devices on account of the high power generated when compared to currently available devices. Thus eliminating the need for the current approach; that is, placement of a battery inside the body, which will eventually be removed when its life-time has ended, subjecting the patient to dangerous and expensive procedures. Table 2.1 lists the state of the art in power generators for energy harvesting [1, 5, 8-15]. These systems are diverse in the source of energy that they convert and in the method used for conversion. But all systems convert some sort of energy (kinetic, thermal, solar, infra-red ultrasonic and radio frequency) into electrical energy by use of a transducer (piezoelectric, electromagnetic, thermoelectric, photovoltaic and resonating circuit). Modern turbine systems are increasingly required to satisfy needs of portable devices, medical, and biomedical systems [16], but the most important goal is improving environmental

compatibility and adaptability without detriment to their performance. There are limitations in the use of micro turbines when the application demands special characteristics such as constant pressure, input and output size and shape, total immersion in a microfluidic system, and adaptability to be used in different positions [7, 17]. Traditional impulse turbines, such as Pelton and Banki [18-21], have a fixed orientation and position, and do not require pressure around the rotor chamber, because the fluid jet is created by the nozzle prior to reaching blades; in general the fluid is in free flow after blades are impacted. To solve problems presented above, a novel mini notched turbine is developed. The system explained in this chapter fulfills a different function compared to the one found in the Banki and Pelton casings, which are used only to protect surroundings from water splashing [22]. The special casing and mini notched blades are designed to optimize the amount of fluid injected at the inlet, contain and control the pressure of working fluid through the turbine, and maintain volumetric pressure on the surface of blades that are not receiving the initial fluid stream directly.

2.3 Mini Notched Turbine Energy Harvesting Source

There are three fundamental components in any energy harvesting system: energy harvesting source, power management circuit with maximum power point tracking system in order to gather maximum power and deliver it to next stage, and a storage device connected to an electrical load as shown in Fig. 2.1.

The harvested power coming from energy harvesting source must be converted to useful DC power form for either uses it directly through the connected load or charge the batteries/Supercapacitors. Appropriate power management circuit is needed between the Energy source and electrical load to achieve maximum power delivered to the load and minimum power loss.

Table 2.1: State of the Art of Energy Harvesting Sources [1, 5, and 8-15].

Energy Source	Power/Energy density	Advantages	Comments
Solar cell/ambient light	100 μ -100mW/cm ²	High power	15-30% efficiency
Thermal	30-50 μ W/ 60-150 μ W/cm ²	-	Low Power
Wireless radio frequency	150 mW	High power	Near a RF transmitter
Kinetic: Blood pressure fluctuations	2.4 μ W	Implantable	Low Power
Wind	1 mW/ cm ²	High power and usable	Average speed
Wireless energy transfer	14 mW/ cm ²	High power	Short distances
Ultrasonic	21.4 nW	No interference	Low Power
Kinetic Foot pressure (Piezo)	1 W	High power	Human dependent
Kinetic: Orthopedic implant pressure	4.8 mW	Implantable	High Power
Cardiovascular pressure and flow	417 μ W	Tested in-vivo	Low Power

2.3.1 Mini Notched Turbine Energy Harvesting Source

Great innovations of the last century have ushered continuous progress in many areas of technology, especially in form of miniaturization of electronic circuits. This progress shows a trend towards consistent increases in memory density, processing speed and power density; and towards a decrease in power requirements due to miniaturization [1]

A lot of power sources can be used in order to provide power to low power applications [2]. Some of them have potential characteristics and can be designed to deliver a maximum power like a mini notched turbine. It is a novel device that can be used for converting flow into

electrical energy by using electromagnetic subsystems to transform kinetic energy into electricity. Mini notched turbine system is shown below in Fig. 2.2.

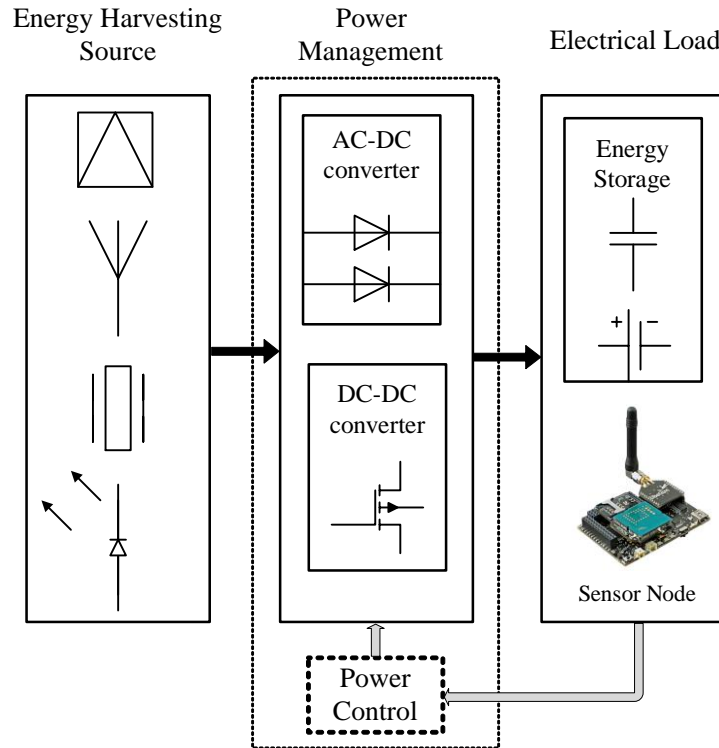


Figure 2.1: Overview of energy harvesting system [23, 24].

The process of energy extraction from the circulatory system using mini notched turbine is possible and this will expand the implementation options to ensure that enough power is obtained to use the system in medical band applications. This is a process of integration through which each part of the system is coupled and optimized for maximum power transfer and efficiency.

This research will make it possible to integrate a power source that converts mechanical energy to electrical energy and uses that energy to supply most of the wireless devices, portable devices and implantable medical devices on account of the high power generated when

compared to currently available devices. Thus eliminating the need for the current approach; that is, placement of a battery, which will eventually be removed when its life-time has ended.

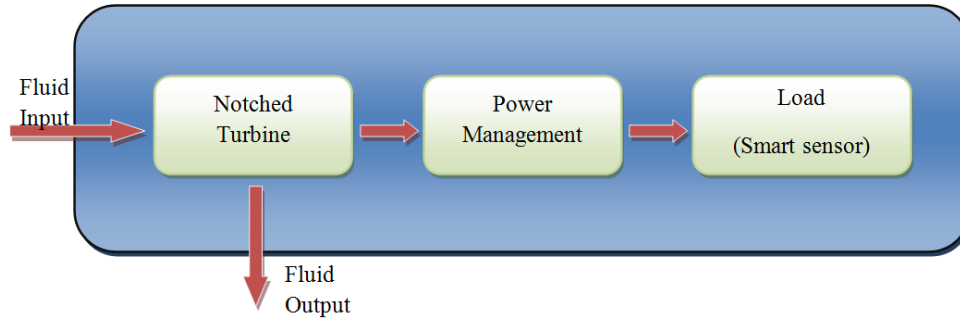


Figure 2.2: Block diagram illustrating proposed integrated mini notched [12].

2.3.1.1 CAD Design

The CAD design and size of the notched turbine is completed based on fundamentals of adaptability, pressure, maximum flow rate, compatibility, and 3D printing capability as well as potential applications [25-28].

2.3.1.2 Rotor Design

The turbine is a new model of impulse turbine with an immersed rotor, which additionally uses reaction characteristics to spin the rotor. The rotor design takes advantage of impulse and reaction turbine designs [29-33] where the impulse spins the turbine resulting in an accelerated flow and removes kinetic energy from the fluid flow. Also, the turbine is designed as a constant pressure turbine that requires a constant flow to work. When blades are initially impacted by the fluid, the direction of the fluid is changed, adding more force that contributes to the continuous spin of the rotor. As part of the turbine reaction benefits, the notch also assures more interaction between the fluid and blades because at the time of jet stream impact on the blade, the notch redirects the fluid and more than one blade is impacted increasing the impulse

force and the angular velocity of blades. Therefore, the notch not only contributes toward increased rotation, but also towards minimizing vortices between blades, thus, guaranteeing the proper circulation of the fluid inside of the rotor chamber and between blades. Blades have a curved profile to increase the blade surface area, which the fluid pressure acts upon. The geometry and rotor design is shown in Fig. 2.3.

2.3.1.3 Overall System

The turbine design, analysis and calculations are conducted with potential applications in mind. The size, shape, and other physical parameters are selected to make sure that the turbine design can be easily adaptable, without modifying the original physical conditions of the system. The inlet/outlet shapes and a scaled size of this turbine are defined for a closed micro fluidic system. The turbine consists of two main parts: the runner or rotor, and the holder or enclosure. The runner has a circular solid center where curved vertical blades are fixed, as is shown in Fig 2.3. The size and design make it very suitable to be developed with a prototyping machine system. The turbine behavior shows that a change in momentum transmits a pressure onto the blade surfaces and produces rotational movement of the blades [11, 12, 19, and 33]. The mini notched turbine has increased efficiency over traditional turbine systems due to changes in the inclination angle of the nozzle and large hub diameter and blade attachment vortices and increasing internal pressure. Therefore, the generated power of the mini notched turbine has been increased by 35% over traditional turbine systems under the same conditions [11, 22, 33-35]. Mini notched turbine approaches with commercial generator are shown with different volumetric sizes in Fig. 2.4.

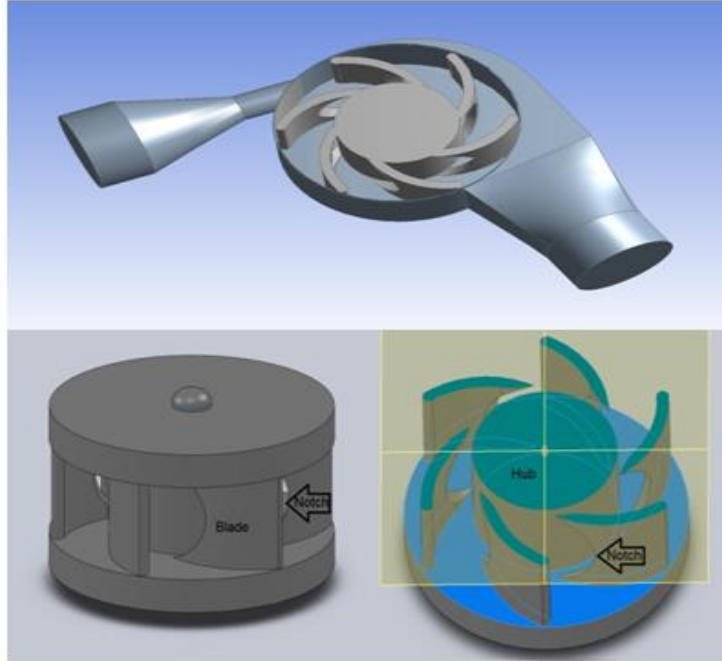


Figure 2.3: Mini notched turbine design [11, 12].

2.4 Mini Notched Turbine Generator

The energy source which converts the flow (air or liquid) into AC or DC power depending on what type of generator (AC or DC) used is investigated within the mini notched turbine energy harvesting system. In this work, the energy harvesting source is mini turbine with notched blades radius directly connected to an AC generator. The power calculations start with quantifying the flow power P_{Flow} using the relationship between nozzle velocity V_n in m/s as shown in Fig. 2.5 below and the potentially available power in flow P_{Flow} can be expressed as [11, 12, 33, and 34]

$$P_{Flow} = \frac{\rho Q V_n^2}{2} \quad (2.1)$$

Alternatively, the power available on a rotor is evaluated using the basic mechanics applied in the rotational system, which states that power available is the product of the torque and angular speed [11, 18].

$$P_R = T_T \omega = T_T \frac{U_1}{r_1} = \frac{\rho Q}{r_1} (V_n U_1 X_1 - U_1^2 X_2) \quad (2.2)$$

where T_T is total torque, ω is angular velocity, U_1 is defined as the tangential velocity on rotor through the turbine, r_1 is distance between the rotor axes and the furthest point of the first blade, and X_1 and X_2 are constants defined in [11]. The maximum mechanical power can be found by differentiating expression (2.2) and expressed as

$$\frac{dP_R}{dU_1} = V_n X_1 - 2U_1 X_2 = 0 \quad (2.3)$$

The maximum mechanical power occurs when:

$$V_n = 2U_1 \frac{X_2}{X_1} \quad (2.4)$$

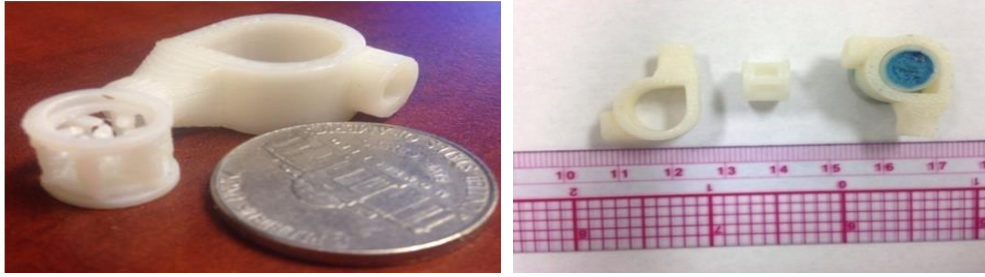
where ρ is fluid density in kg/m^3 , (1 for water and 1.2 for air) and Q is volume flow rate in ml/min .

The hydromechanical efficiency of mini notched turbine (η_{Hy}) is defined when the potential fluid energy is transformed into mechanical energy taking into consideration the losses. Hydro-mechanical efficiency is the ratio of the mechanical rotor power to the potentially available power in fluid P_{Flow} and can be written as [8, 11, 25, and 26]

$$\eta_{Hy} = \frac{P_R}{P_{Flow}} = \frac{2(V_n U_1 X_1 - U_1^2 X_2)}{r_1 V_n^2} \quad (2.5)$$

and maximum mechanical efficiency can be written as

$$\eta_{HyMax} = \frac{P_{RMax}}{P_{Flow}} = \frac{2T_T \omega}{V_n^2 \rho Q} \quad (2.6)$$



(a)



(b)



(c)



(d)

Figure 2.4: Different mini notched turbine approaches with volumetric size of; a) $27*27*6$ mm^3 , b) $41.8*41.8*14.1$ mm^3 , c) $41*41*8.5$ mm^3 , and d) $46.8*43.8*12.4$ mm^3 [12].

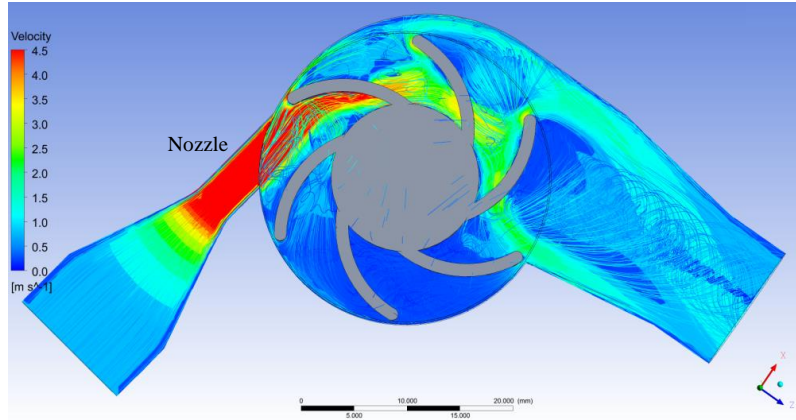


Figure 2.5: Nozzle velocity simulation [11, 12].

The performance of notched turbine generator in power aspect is shown in Fig. 2.6. The flow power P_{flow} , the mechanical rotor power P_R , and the transformed electrical power P_E using AC generator. Based on calculation in [11], the experimental hydromechanical efficiency of the mini notched turbine is 53% (60.23% in simulation) with a 5000 ml/min flow rate and the maximum hydromechanical efficiency is 75% [11]

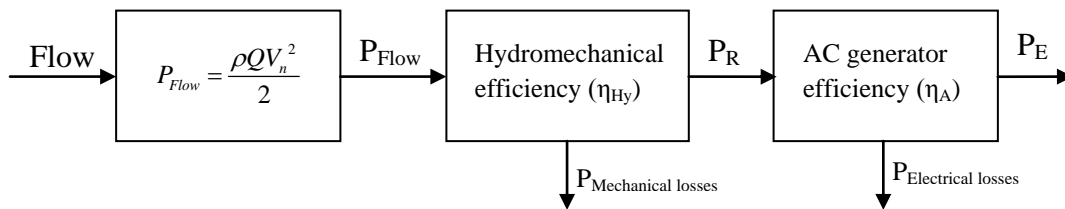


Figure 2.6: Block diagram of mini notched turbine [11, 12].

The electrical power P_E is obtained experimentally from the mini notched turbine shown in Fig. 2.7 using air flow over a range of flow speeds of 250-2500RPM and different flow rates. The power curves of the mini notched turbine are shown in Fig. 2.7 where these curves are calculated with different resistance loadings with three different sizes of MiNT and different

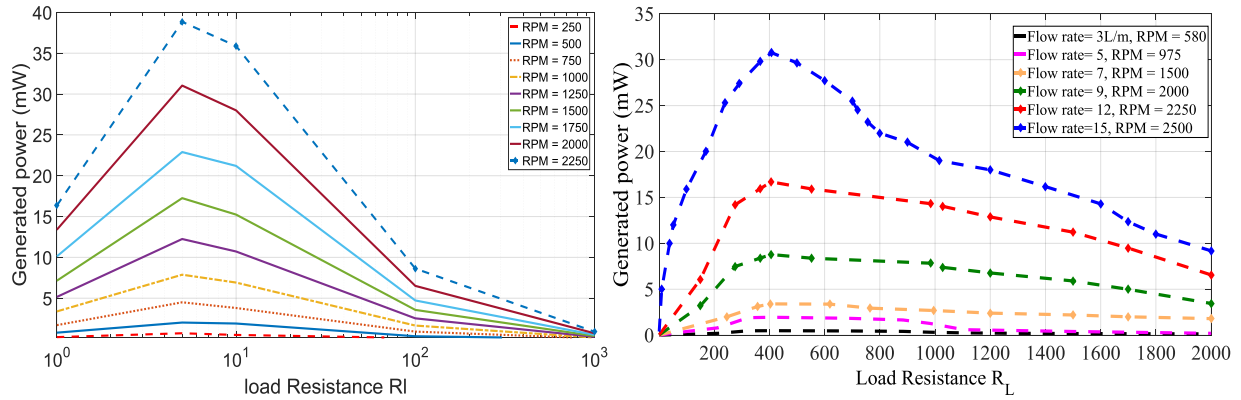
generators to clearly demonstrate the mini notched turbine characteristics. It can be easily observed from Fig. 2.7 that the generated electrical power ranges from 0.5 mW to 92 mW. For the average flow speed at 1500 RPM, the electrically power generated is 17 mW which is enough to power most small electronic devices. The generated power curves in Fig. 2.7. show that the mini notched turbine maximum generated power (maximum efficiency point) over a range of flow speed levels and different flow rates can be reached with optimum load impedance [19, 36].

Fig. 2.8 shows the generated power from mini notch turbine varies as a function of output voltage for different flow speeds and shows that, for any given flow speed, there is an optimal output voltage where the generated power is maximized. The output voltage of mini notched turbine is in the range of 0-1V and the maximum generated power is 38.8mW [19, 36].

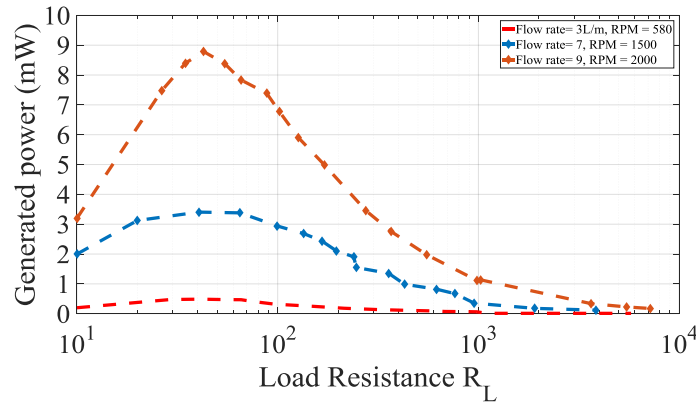
Fig. 2.9 shows I - V characteristics and measurement results of the mini notched turbine used to calculate load impedances that maximize the generated power at different flow speeds. These impedances will be used later in the optimization in order to improve the total efficiency of the power management circuit. Generally, for any flow speed, there is an optimum value of load where the power generated by notched turbine is maximized.

Mini notched turbine differs from other turbine models in three main ways. First, the design makes it possible for the turbine to be immersed in a dynamic fluid, and be able to work in different positions and orientations. Second, the preferred embodiment of the turbine rotor utilizes a new blade curvature and shape, in addition to a semicircular notch on the internal proximal edge of each blade, to aid in the fluid redirection and allows a continuous circulation of fluid inside the rotor chamber. Third, the casing, coupled with notched blades, optimizes the flow of the fluid injected at the inlet and prevents drastic alterations and changes in pressure of the

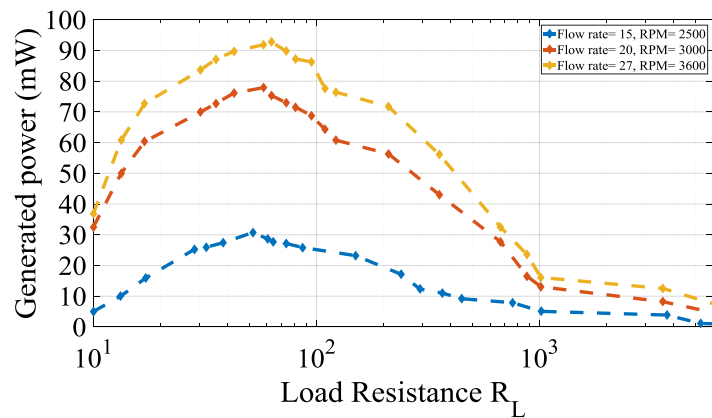
working fluid through the turbine, thus maintaining volumetric pressure on the surface of blades that are not directly impacted by the initial fluid stream.



(a)



(b)



(c)

Figure 2.7: Power curves of MiNT generator over a range of flow speeds and different resistance loadings. a) Two MiNT approaches with different speeds, b) low power range, c) high power range [12].

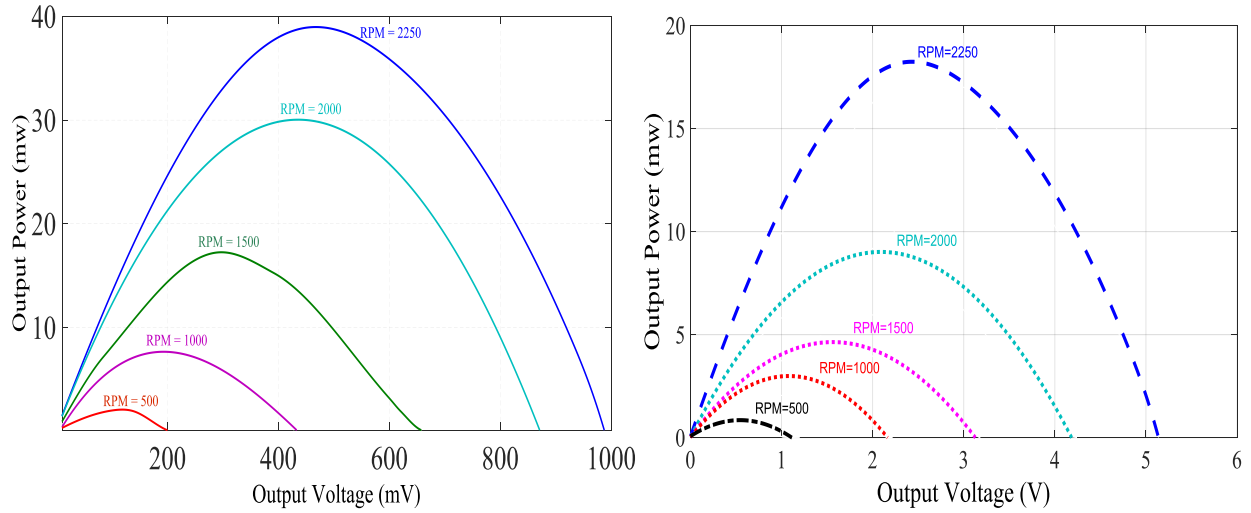


Figure 2.8: Measured generated power against output voltage for two MiNT approaches [19, 36].

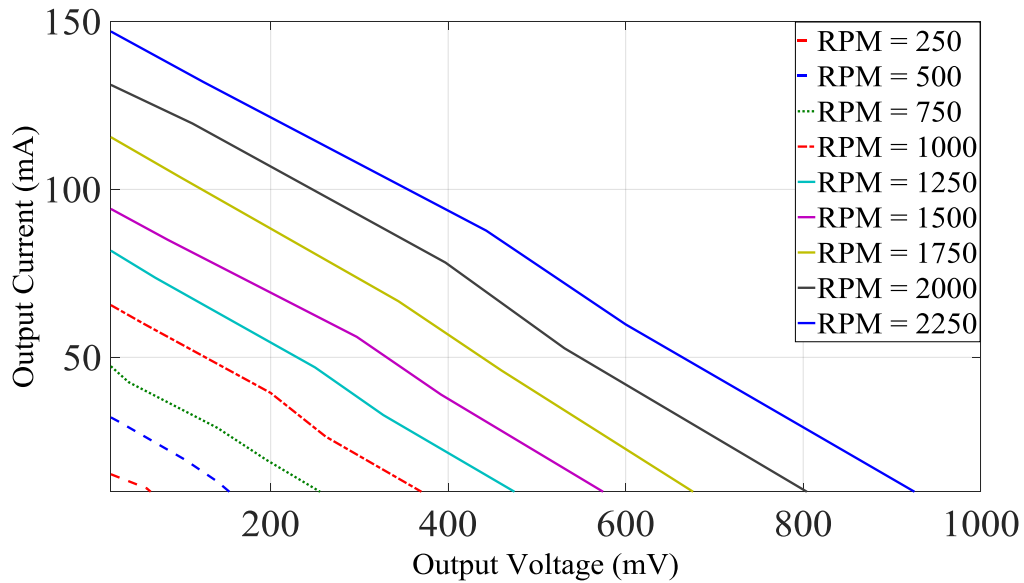


Figure 2.9: Measured I-V characteristics of mini notched turbine for different flow speeds [19, 36].

2.5 RF Energy Harvesting Source (Rectenna)

For many years, RF wireless harvesting systems have been investigated, but only a few of RF sources have been able to generate sufficient energy that can be used as feasible source for low power electronic devices like RF rectenna, it could provide unlimited energy for the lifespan of these devices [6, 24, 37-39].

2.5.1 Introduction

The need for ultra-low power for standalone embedded systems that need to operate for very long periods of time is growing rapidly. Requirements in this market for low power and long life are pushing the limits of current technologies using RF energy sources and existing solutions that may be applicable to low power applications.

Therefore, new techniques and creative designs are required to meet urgent requirements of today's cutting-edge low power devices. RF energy harvesting systems are increasingly required to satisfy the needs of wireless systems [6], but the most important goal is improving environmental compatibility and adaptability without detriment to their performance. Power sources for biomedical applications using RF wireless harvesting systems have gained considerable attention recently [40-46], such as in inductive coupling [45], capacitor coupling [45], magneto dynamic coupling [46], and far- field radio frequency methods such as the rectenna. These methods can be used for longer distances applications. Rectenna currently has gained considerable attention to be used as power source for implantable or wireless medical devices. This is because the rectenna can easily be integrated with microwave integration circuits, has low cost, and small volume. Recently, most of the research on the design of implantable rectennas has focused on issues related to compact size, biocompatibility, power efficiency, and the life span of implantable medical devices.

2.5.2 Background

Far-field RF technique has been used for almost 40 years to power small systems remotely such as smart sensors and large systems such as unmanned aerial vehicles [47]. In order to power these systems effectively using RF energy source, radiated power, a polarization of the RF source, and optimal line-of-sight between the transmitter and receiver should be taken

into consideration. The power efficiencies of most RF rectennas introduced in literature review have been measured using known RF sources rather than using natural RF energy to harvest energy [48]. Recently, some of the research on design of RF rectennas has highest conversion efficiency, the power efficiency is 90% in [49], 78% in [50], and 60% is achieved in [51]. However, these high efficiencies have been measured with high input RF power. The conversion efficiency of RF rectenna's designs is listed in Table 2.2, [52].

A group of rectennas can be combined together in order to increase the surface area to increase input RF power and conversion efficiency [24, 38, 39, and 53-57]. Also, a broadband antenna is another good method in order to harvest energy over a wide range of RF frequencies [57, 58]. However, one major drawback with this method is that broadband rectennas have lower conversion efficiency at a given frequency compared to RF rectenna designed for specific center frequency. At lower input RF power levels, the conversion efficiency has been decreased due to the forward voltage of Schottky diodes, distance, path loss, and antenna gain. This makes it difficult for a rectenna design.

2.5.3 RF Rectenna

Great innovations of the last century have ushered continuous progress in many areas of technology, especially in the form of miniaturization of RF energy sources. This progress shows a trend towards consistent increases in power density, and towards a decrease in power requirements due to miniaturization and consumption power [1].

A lot of RF energy sources can be used in order to provide power to low power applications [2]. Most of them have potential characteristics and can be designed to deliver a maximum power like rectenna. It is an antenna with rectifier device can be used for converting electromagnetic energy into electrical energy. As shown in Fig. 2.10, Most of rectenna designs

consist of three basic parts: an antenna, matching network to maximize the power delivered to the load, and a rectifier circuit.

The main component of the rectification process is Schottky diode which is less power consumption, faster switch, and less voltage drop than regular diodes. The selection of Schottky diode depends on forward voltage, power requirements, I - V characteristics as described in expression (2.7) as shown below, and maximum reverse breakdown voltage, current voltage characteristics is defined as [64]. In this work, the voltage doubler using two high frequency Schottky diodes is used.

$$I_D = I_S \left[e^{\frac{V}{NKT}} - 1 \right] \quad (2.7)$$

where I_D is diode current, I_S is reverse saturation current, V is forward bias voltage, K is Boltzmann constant, T is absolute temperature, and N is ideality factor.

Since the rectenna will be used in future work for biomedical devices, operating frequency was chosen to be 2.4 GHz and the material used in antenna design could be biocompatibility material such as Silicon Carbide (SiC) or coated with biocompatibility material. In this work, the antenna was designed using Roger RO4350B material and it will be coated later, it is easy to integrate and fabricate and has low loss feature and this could maintain the power efficiency. Matching network is the next step in the design to achieve maximum power delivered and minimum return loss (S_{11}) [37].

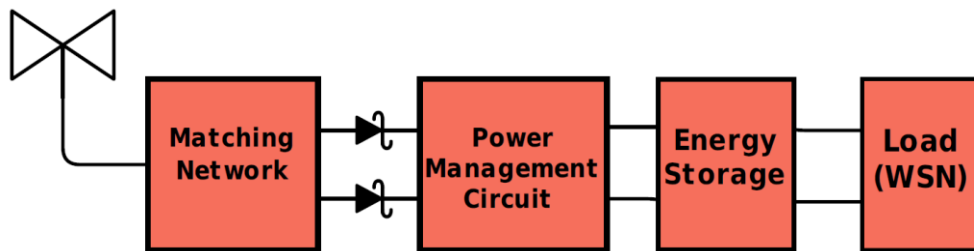


Figure 2.10: Block diagram of RF energy harvesting system.

Many studies have been performed on the amount of generated power from rectenna such as [23, 24, 38, 39, and 65] which showed the generated power range from (10 μ W) to (1W) but this power range varies with distance, path loss, antenna gain, and frequency. The efficiency of rectenna is measured by *RF-DC* ratio as shown below.

$$\eta_{\text{RF-DC}} = \frac{P_1}{P_{\text{RF}}} \quad (2.8)$$

$$P_{\text{RF}} = P_{\text{density}} * Ae \quad (2.9)$$

$$Ae = \frac{\lambda^2 G}{4\pi} \quad (2.10)$$

where P_{density} is power density, P_1 is output power of rectenna, Ae is the effective area for patch antenna for example, λ is wavelength, and G is antenna gain. Note that the effective area of the patch antenna is larger than the physical area because of fringing field effect and typically it trimmed by 2-4% to achieve resonance at the desired frequency [37, 66]. In order to calculate the effective area of patch antenna, expressions (2.11-2.13) are used to calculate the actual (L_p) and effective (L_{eff}) length of patch antenna [67].

$$L_p = L_{\text{eff}} - 2\Delta L \quad (2.11)$$

$$L_{\text{eff}} = \frac{c}{2f\sqrt{\epsilon_e}} \quad (2.12)$$

$$\Delta L = 0.412h_p * \frac{\left\{ \left(\epsilon_e + 0.300 \right) * \left(\frac{w}{h_p} + 0.264 \right) \right\}}{\left\{ \left(\epsilon_e - 0.258 \right) * \left(\frac{w}{h_p} + 0.813 \right) \right\}} \quad (2.13)$$

where ΔL is the extended patch length, c is the speed of light, f is the operating frequency, ϵ_e is the effective dielectric constant, h_p is the height of the patch, and w is the width of the patch.

2.5.3.1 Antenna Design

The antenna is a device that used to transmit and receive electromagnetic waves. Antennas were originally introduced in 1842 by Joseph Henry, Professor at Princeton, NJ. Henry discovered that the current in a parallel circuit has magnetic properties by sending a spark to a circuit. Also, Henry detected flashes away from his house after done other experiments. In 1875, Edison found out that the key-clicks could radiate. Later in 1885, Edison patented a complete communication system using different types of antennas. In 1882, A. E. Dolbear used similar antenna system for transmitting codes to significant ranges. In 1887, H. Hertz built an antenna system that could transmit and received radio waves. A balanced antenna connected to an induction coil was used as a transmitter. Later on, H. Hertz established the principles of antenna polarization [68].

2.5.3.2 Matching Network

Matching network between the antenna and rectifier circuit is used to achieve maximum power efficiency and minimum return loss (S_{11}). However, the input impedance of rectifier changes for different input power levels, because of the nonlinear I - V characteristics of diodes [66, 69-75].

The nonlinear behavior of diodes impedance and characteristics of the matching network are commonly designed based on the specific characteristic impedance of antenna, specifically center frequency, and specified input power level in order to maximize the power delivered to the load [66, 72, 76, and 77]. Several rectifiers with known rectifying characteristics, such as voltage doubler could be connected in parallel at different input power levels in order to expand the RF applications of the rectenna [51, 78].

Table 2.2: Comparison of Conversion Efficiency in Different Configurations of Rectenna [59].

Antenna type	Input power	Load Resistance (Ω)	Frequency (GHz)	Efficiency ($\% \eta_{RF-DC}$)	Reference
Square aperture coupled patch	10 μ W-100 μ W	8200	2.45	15.7-42.1	[40, 60]
Patch	120mW	100	35	29	
Aperture coupled stacked microstrip	100 μ W	9200	2.45	34	[61]
Dipole	135mW	400	35	39	
Patch	251mW	220	2.45	40.1	[62]
Coupled microstrip rings	10mW/cm ³	150	5.8	73.3	
Step dipole	100mW/cm ³	250	5.8	76	
Microstrip circular sector antenna	10mW	150	2.4	77.8	[50, 52]
Patch	1 μ W-1W	2400	0.9-2.45	80	[50, 51]
Dual rhombic loops	2mW/cm ³	150	5.8	82	
Dipole	50mW	327	5.8	82	
Dipoles	2.48-8.77 mW/cm ³	310	2.45 & 5.8	82.7-84.4	
π-shaped radiator with a stacked and spiral structure	12.5mW	5000	0.433 & 2.45	86	[40, 50, and 63]

The enhanced maximum power point tracking system is a good alternative method in order to enhance the power efficiency when the input RF power is relatively low [24, 79, and 80]. Common passive matching networks utilized for RF energy harvesting applications include discrete passive networks such as *LC* networks, microstrip lines, and stub sections as shown in Fig. 2.11. The matching network was designed based on the load impedance, source impedance, and the specifications of Schottky diodes and then optimized using built-in optimization tool in Advanced Design System (ADS), DC block capacitor and smoothing capacitor were added to the design. Additionally, the microstrip lines were fabricated using Roger RO4350B [81], (dielectric constant $\epsilon_r= 3.48$ and tangent loss $\tan\delta= 0.0037$).

2.5.3.3 Rectifier Circuit

One of the most important components in the rectenna RF energy harvesting system is rectifier circuit. Many of the researchers have demonstrated that the conversion RF-DC efficiency of the rectenna is influenced by the characteristics and equivalent model of the Schottky diodes [82-84]. A good Schottky diode is usually chosen based on low forward voltage, low saturation current, low parasitic inductance and capacitance, low series resistance, high frequency performance, lower junction resistance, and low reverse bias voltage. Schottky diode impedance can be determined using equivalent circuit model as shown in Fig. 2.12, where C_p and L_p are the diode's parasitic capacitance and inductance respectively, R_s is series resistance, R_j is junction resistance, and C_j is junction capacitance. This equivalent model circuit is used for designing the matching network at given input power because R_j and C_j are bias dependent. Table 2.3 lists some commercial Schottky diodes available in the market and their parameters [85].

2.5.4 Fabricated RF Rectenna

Fig. 2.13 shows a fabricated RF rectenna at 2.4 GHz on Roger RO4350B [81] printed circuit board using a milling machine. The matching network is realized with microstrip lines to ensure maximum efficiency and minimum power loss. Signal generator connecting to 2.4 GHz monopole antenna was used as a power source in order to harvest energy by RF rectenna in Center for Wireless and Microwave Information Systems lab at University of South Florida (WAMI Lab).

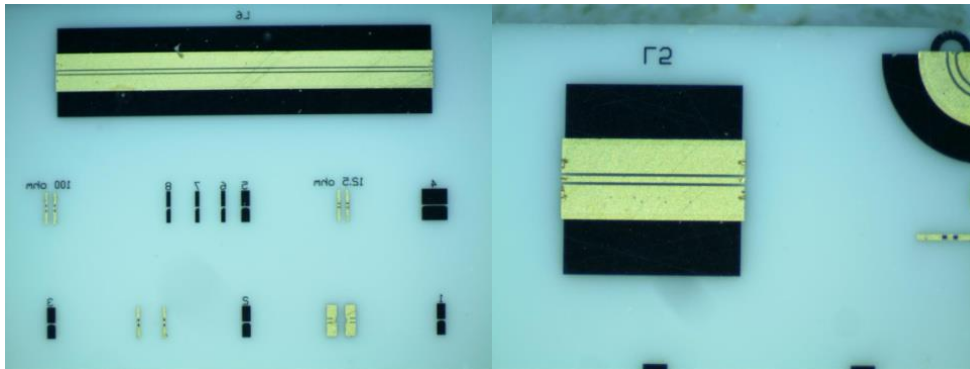
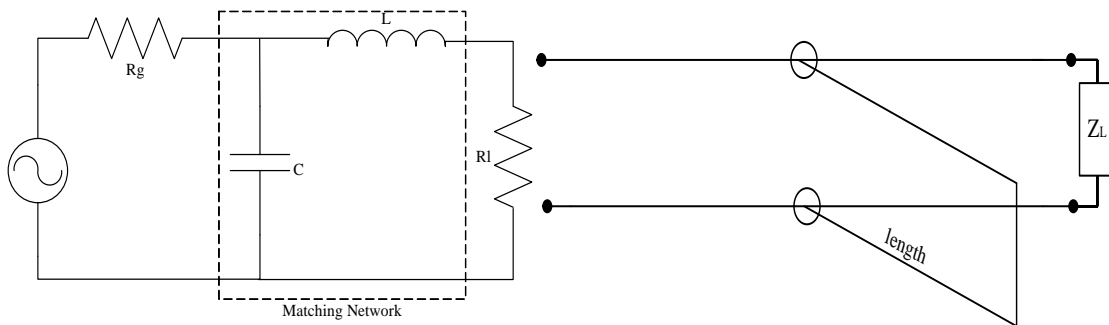


Figure 2.11: Matching network techniques.

The generated power curves in Fig. 2.14 show that the rectenna maximum generated power (maximum efficiency point) over a range of input power levels can be reached with the optimum load impedance. For the rectenna designed, this resistance is 400Ω . Based on that, the rectenna was designed and fabricated. Fig. 2.15 shows the power measurements obtained experimentally from rectenna comparing with simulation results over a range of power received

by the antenna with different load impedances. It is observed that the efficiency is about 70% (75% simulation).

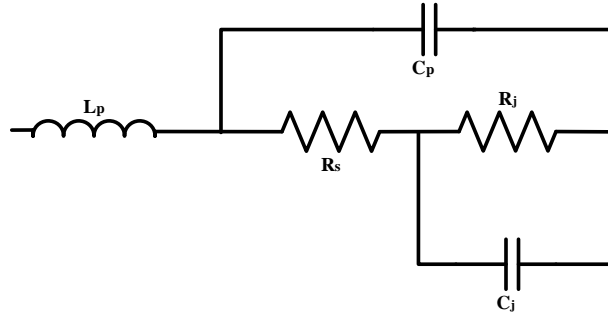


Figure 2.12: Equivalent circuit model of Schottky diode.

Good agreement between results obtained from simulation and the measurement is observed. The differences between the measurement results and the simulation ones could be due to the discontinuity effects, the connectors, the fabrication process, losses, and measurement errors.

Table 2.3: Commercial Schottky Diodes [85].

Schottky diode	R_s (Ω)	L_s (nH)	C_j (pF)	C_p (pF)	I_s (μ A)
SMS7630	20	0.05	0.14	0.005	5
SMS1546	4	1	0.38	0.07	0.3
MA4E2054	11	N/A	0.1	0.11	0.03
HSMS-286	6	2	0.18	0.08	0.05
HSMS2800	30	N/A	1.6	N/A	0.03

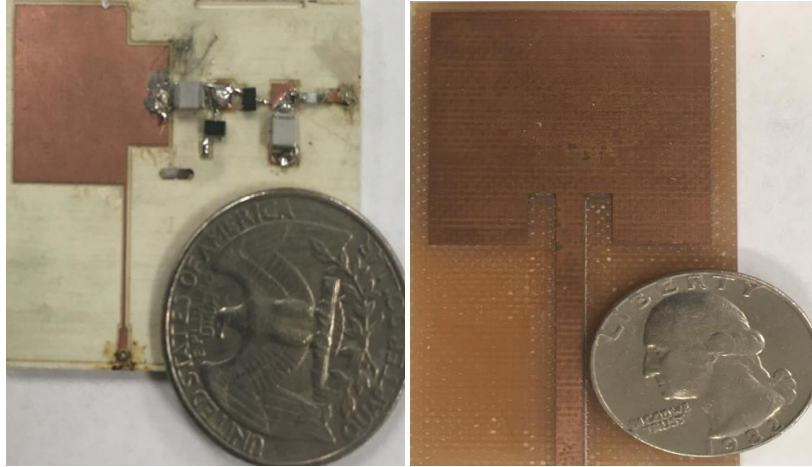


Figure 2.13: Fabricated rectenna with matching network and rectifier stage.

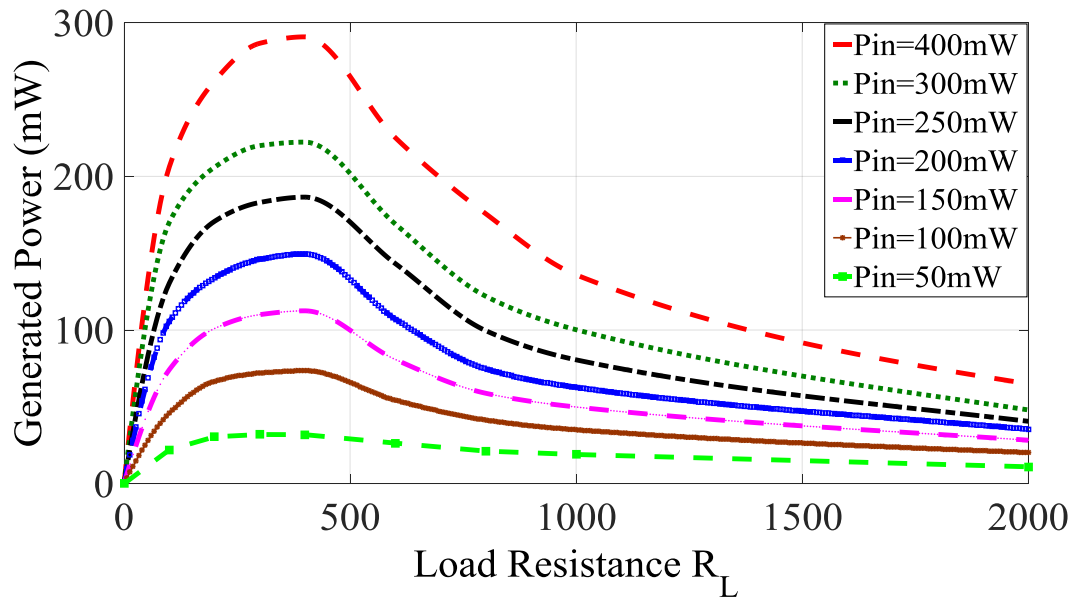


Figure 2.14: Simulation results of power generated by rectenna over a range of input power for different loads.

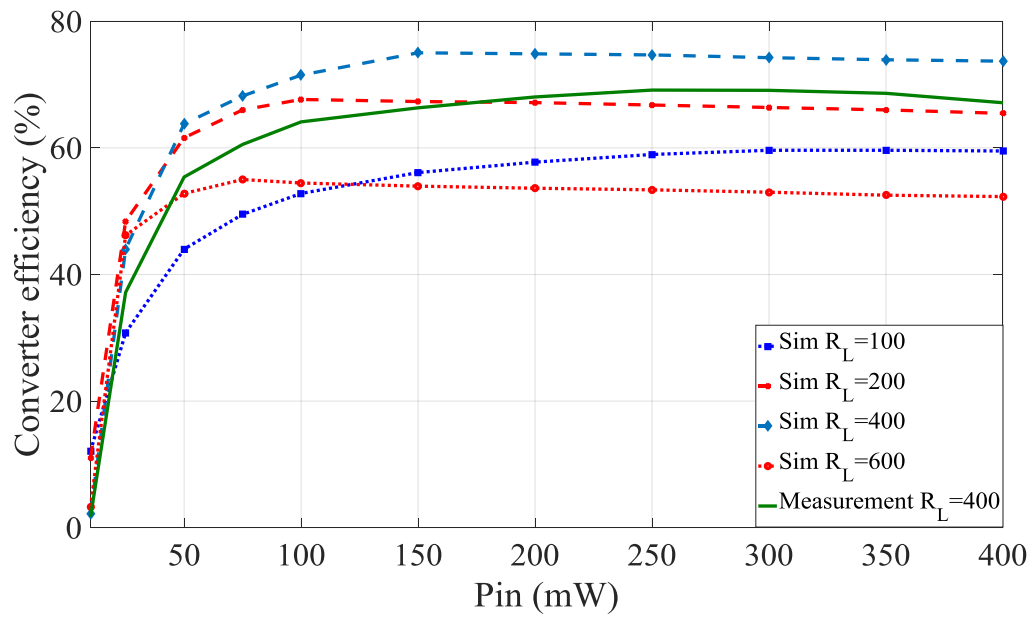


Figure 2.15: Measurement and simulation results for the efficiency of rectenna.

CHAPTER 3:

OVERVIEW OF POWER MANAGEMENT CIRCUITS

3.1 Introduction

A power management system indicates the control, power efficiency, and generation of regulated voltages needed to operate electronic devices. Today, electronic systems require a power source to be combined with a power management design to enable high power efficiency. Switching regulators, switched capacitors, linear regulators, and voltage DC-DC/AC-DC converters are fundamental parts of a power management system. Recently, the design trend is towards bringing down the standard voltage from ± 15 V to 3.3 V and 1.8V [23, 24, and 35]. This is because of the needs for high speed integrated circuits and nano scaled systems. Based on Moore's law, the scaling of transistors used in the fabrication implies lower thermal voltages which indicate lower voltage bias. The availability of energy and dissipation of power in electronic devices and low power applications where the energy harvesting technique is used to provide power are not steady over time. Therefore, a power management system becomes a viable technique to maintain high power efficiency and minimize the energy consumption. This chapter presents an enhanced power management circuit design for harvesting maximum power from energy harvesting sources with input power in the range of milliwatts. This design improves the efficiency of optimized power management circuit by 7% comparing with conventional power management circuits over a wide range of input power, allowing harvesting more power from energy sources and delivering it to the load.

In energy harvesting systems, the performance depends on the operating conditions such as I - V characteristics. Therefore, the amount of maximum power harvested from the energy source depends on energy source profile (temperature, flow, wind,...), and load characteristics such as impedance.

3.2 Maximum Power Point Tracking System

Energy harvesting systems should be implemented in a certain way to achieve maximum power efficiency for any input power level at all times. When an energy source is connected directly without power management circuit to the load, the energy harvesting generator will operate on the I - V curve, but far away from maximum power tracking point (MPPT) [23, 24, 35, 38, and 39].

In order to make the system operate close to MPPT point and enhance the power efficiency, a DC-DC converter can be integrated between the energy harvesting system and the load as shown in Fig. 3.1, which can operate as impedance matching between them. Also, it can efficiently deliver the energy to the storage device/load. These DC-DC converters are normally used as natural impedance matching to track maximum power point. The main idea of using MPPT is to track the MPP and ensure that the power management system extracts the maximum input power and transfer it to energy storage/load. Based on that, a methodology for optimizing ultralow power management circuit to improve the efficiency of DC-DC converter is proposed in this work, this is accomplished using particle swarm optimization technique, where the converter efficiency is used as the fitness function and inductor and on-time are chosen as optimized parameters. This design improves the DC-DC converter efficiency and the efficiency of power management circuit by 10%.

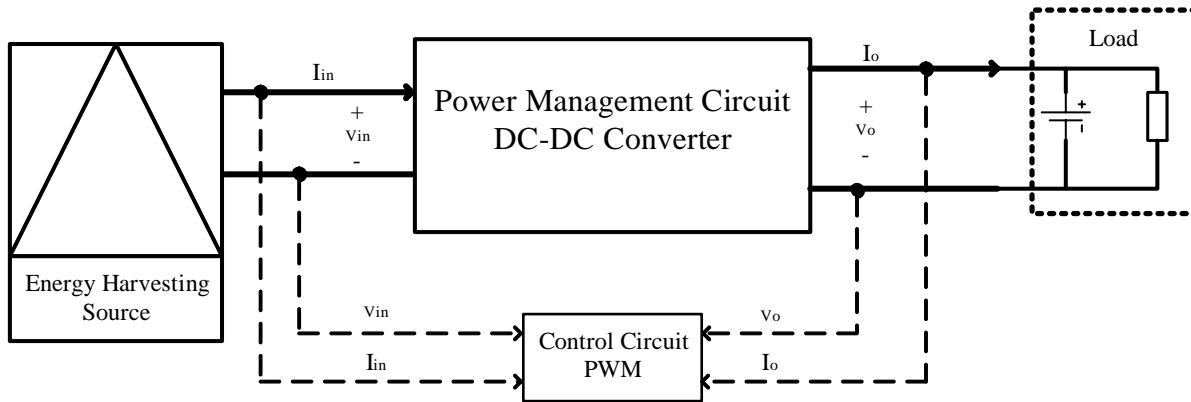


Figure 3.1: Energy harvesting system using DC-DC converter as matching impedance.

Integrating DC-DC converter in the power management circuit of the energy harvesting system is to 1) step up/step down the DC voltage level coming out of the energy source in order to charge supercapacitor or rechargeable battery, 2) track the maximum power point (MPP) in order to transfer maximum power to the load by acting as matching network between the source and the load. There are different techniques proposed to find the maximum power point. In [86], the MPPT model is designed based on characteristics of photovoltaic systems where the irradiance is the key for seeking maximum power point as well as the flow speed is the key maximum power transfer for large-scale wind turbine [87]. Many techniques, such as an open-circuit voltage technique [88-93], short-circuit technique [88, 94, and 95], feedback voltage and current technique [96, 97], differentiation technique [98, 99], sampling technique, perturbation and observe (P&O) technique [100-105], and conductance incremental technique [106] have been proposed to track maximum power point. The MPPT techniques can be divided into direct and indirect methods according to [88]. The direct method uses many iterations searching for the MPPs. However, the energy loss of the energy harvesting source that uses direct methods is high because of the system is constantly searching for MPP. The direct method is not suitable for mini

notched turbine system. The indirect methods use the parameters and data of energy harvesting systems in advance such as I - V characteristics of energy source, power curves of energy source generator for different flow rates or RF power, or the data obtained from mathematical models to predict the MPP. Open-circuit voltage technique, short-circuit technique, and look-up table technique are examples of indirect method.

3.2.1 Resistor Emulation Technique Using DC-DC Converter

The main concern of researchers these days is the limitation of a lifetime of the battery where the power consumption is the major factor that degrades the performance of low power applications. Therefore, the need for high power efficiency makes the research in MPPT very valuable as the tracking the MPP using a power management circuit usually determines the maximum power transfer and lifetime of the system.

Most of the current MPPT techniques are not applicable for the mini notched turbine system. An enhanced MPPT technique is proposed in this chapter based on using DC-DC converter as natural impedance matching between the source and the load. This technique is called resistor emulation. It was used for the first time by Khouzam [107] in 1993, Paing et al [24, 38, and 39] used this concept to design MPPT with RF rectenna.

This approach uses the data of I - V curves and power curves plotted in Fig. 2.4, the power curves show the maximum power points occur when the load impedance equals to input impedance. In mini notched turbine and RF rectenna, the source impedance that will be used in MPPT design is 400Ω . When the input impedance matches the load impedance of the mini notched turbine system, the harvested power (power efficiency) is always maximum for various flow rates. However, when the load impedance is higher/lower than the input impedance, the harvested power being generated goes down significantly. MPPT using resistor emulation is a

suitable preference to track and find the MPP and achieve the maximum power efficiency of energy harvesting system.

K. Khouzam [107] presented the resistor emulation by selecting optimum parameters of the energy harvester and the load in order to match perfectly between them. Paing et al. in [38, 39] proposed a boost DC-DC converter to act as resistor emulator between the source and the load where the selection of parameters of boost DC-DC converter is the key design for matching impedance to predict MPP. The proposed MPPT approach increases the power efficiency by 10% comparing to Paing approach [38, 39], where the selection of parameters of boost DC-DC converter was optimized using particle swarm optimization technique to lower the power loss in power management circuit and enhanced power efficiency without adding more components or microcontroller. Moreover, the new approach minimizes the PCB footprint which is crucial in low power applications where the physical size is restricted.

3.2.2 Overview of Boost DC-DC Converter

The boost converter is a well-known DC-DC converter that produces an output voltage higher than an input voltage and steps down the output current. It is a switched mode converter where MOSFET, diode, and inductor are the primary components in boost converter as shown in Fig. 3.2. When the MOSFET is on, the inductor is connected directly to ground as shown below in Fig. 3.3, where the expressions of inductor voltage and the current through the output capacitor can be written as [108]

$$V_L = V_s \quad (3.1)$$

$$i_c = \frac{-V_R}{R_{load}} \quad (3.2)$$

When the MOSFET is off, the inductor will be connected directly to the output as shown in Fig. 3.4, where the expressions of inductor voltage and the current through the capacitor can be written as

$$V_L = V_s \quad (3.3)$$

$$i_c = i_L - \frac{V_R}{R_{load}} \quad (3.4)$$

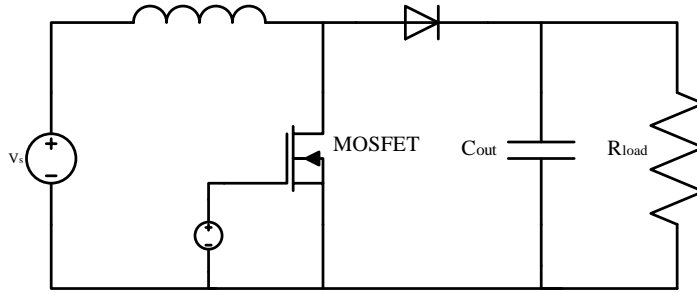


Figure 3.2: Boost DC-DC converter configuration.

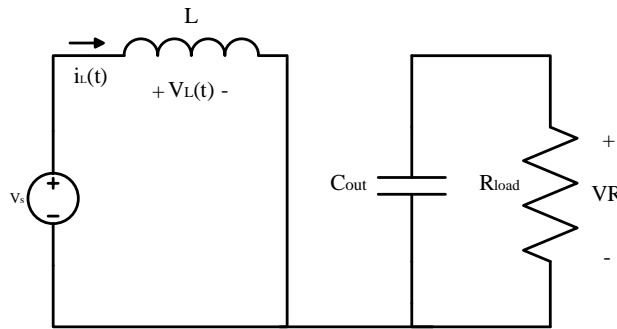


Figure 3.3: Boost DC-DC converter circuit when the MOSFET is on.

Based on the analysis in [108], the output voltage of boost converter is

$$V_R = \frac{V_s}{1-D} \quad (3.5)$$

where D is the duty cycle and always less than 1. In an ideal case, the voltage across the load V_s increases and tends to be infinity when D increases and tends to be 1. However, the power loss of switches and other components limits the voltage.

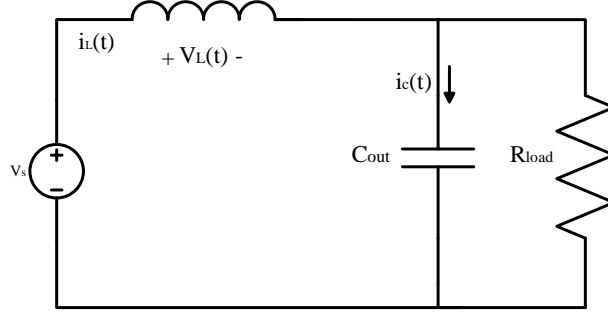


Figure 3.4: Boost DC-DC converter circuit when the MOSFET is off [108].

3.2.2.1 The Discontinuous Conduction Mode

Due to the practical behavior of switches of a boost DC-DC converter, one or more operation modes known as discontinuous conduction mode or critical conduction mode can happen. The discontinuous conduction mode happens when the ripple current in the inductor is large enough to change the polarity of applied voltage. In other words, the switching period is larger than the on-time and off- time of MOSFET as shown in Fig. 3.5 [108].

In first period (D_1T_s), when the MOSFET is on and the inductor voltage is connected to the source, the current coming from the source starts to flow in the inductor, based on expression (3.1), the inductor current is

$$i_L = \frac{V_s}{L} = \frac{V_L}{L} \quad (3.6)$$

In the second period (D_2T_s), where the MOSFET is off and the voltage across the inductor is the difference between the source voltage and output voltage, the diode keeps conducting until inductor current goes to zero. In the third period (D_3T_s), the inductor current is zero and after the third period, the cycle is repeated again. According to Fig. 3.5, the peak current can be expressed as [108]

$$i_{peak1} = i_{peak2} = \frac{V_s D_1 T_s}{L} = \frac{-(V_s - V_R) D_2 T_s}{L} \quad (3.7)$$

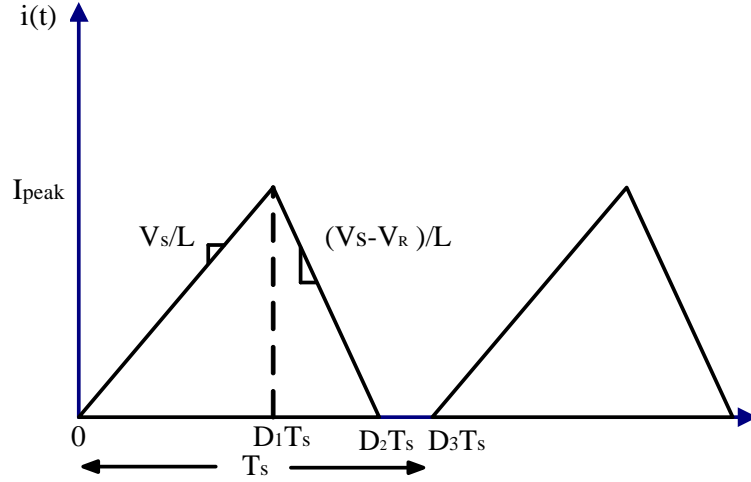


Figure 3.5: The waveform of inductor current [108].

The time where the current of the inductor is larger than zero is

$$D_1 T_s + D_2 T_s = (D_1 + D_2) T_s \quad (3.8)$$

where $D_1 T_s$ is the period of time when the MOSFET is on and $D_2 T_s$ is the period of time when the MOSFET is off. Based on expression (3.7), the duty cycle of the first period is

$$D_1 = \frac{V_R - V_s}{V_s} D_2 \quad (3.9)$$

In order to find the input power of the boost DC-DC converter, the average input current is needed, the average current can be written as [108]

$$I_{i,average} = \frac{i_{peak1}(D_1 + D_2)}{2} \quad (3.10)$$

After substituting expressions (3.7) and (3.9) into expression (3.10), the average current can be written as

$$I_{i,average} = V_s \frac{D_1^2 T_s}{2L} \left(\frac{V_R}{V_R - V_s} \right) \quad (3.11)$$

The input power of the boost DC-DC converter is

$$P_{input} = V_s * I_{i,average} \quad (3.12)$$

Substituting expression (3.9) into (3.10), the input power is

$$P_{input} = V_s^2 \frac{D_1^2 T_s}{2L} \left(\frac{V_R}{V_R - V_s} \right) \quad (3.13)$$

Based on CMOS VLSI design for low power applications and the probability of DC-DC boost converter can be switched on and off to DCM mode based on the power available coming to the DC-DC boost converter, a switching factor will be added to input power expression where it is going to be between 0 and 1. So, the input power can be rewritten as [38, 39, and 108]

$$P_{input} = V_s^2 \frac{D_1^2 T_s \alpha}{2L} \left(\frac{V_R}{V_R - V_s} \right) \quad (3.14)$$

3.3 MPPT with Resistor Emulation Technique Using Boost DC-DC Converter

Energy harvesting systems should be implemented in a certain way to achieve maximum power efficiency for any input power level at all times. In order to make the system operate close to (MPPT) and enhance the power efficiency, a boost DC-DC converter can be integrated between which can operate as impedance matching between them. Also, it can efficiently deliver the energy to the storage device/load. Boost DC-DC converter is normally used as natural impedance matching to track maximum power point where the parameters of boost DC-DC converter are the main factors for calculating the power efficiency. It can be expressed as [23, 38, and 39].

$$\eta_{converter} = \frac{P_{output}}{P_{input}} * 100\% = \frac{V_R / R_{load}}{V_s * I_{i,average}} * 100\% \quad (3.15)$$

The MPPT system using boost DC-DC converter design with resistor emulation technique is shown in Fig. 3.6. Basically, it is composed of boost DC-DC converter to transfer

power efficiently from source to load and control circuit. The optimum value of resistance where the boost DC-DC converter will work effectively is equal to input resistance of energy harvester source (400Ω in RF rectenna energy source). This resistance can be written using expression (3.12) as

$$R_{optimum} = \frac{V_s^2}{P_{input}} = \frac{2L}{D_1^2 T_s \alpha} \left(\frac{V_R - V_s}{V_R} \right) \quad (3.16)$$

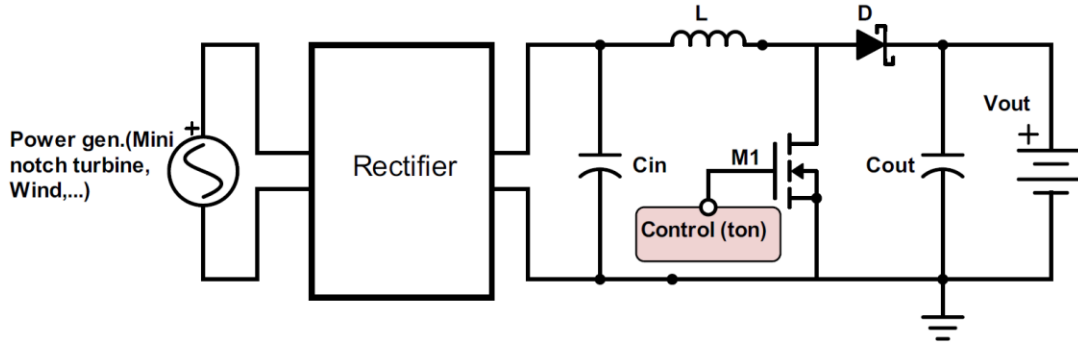


Figure 3.6: Maximum power point tracking system using boost DC-DC converter

According to expression (3.16), the optimum resistance depends on four parameters in order to match the input impedance to output impedance and transfer maximum power to the load. The particle swarm optimization technique is used to optimize and find best values of some of these parameters in order to achieve maximum power transfer and enhanced the power efficiency. The optimization process depends on the power loss models and the value of input resistance where higher values of input resistance mean larger solution space.

3.3.1 Power Loss Analysis

A detailed analysis of the power loss of boost DC-DC converter is presented. These power loss models include: i) conduction losses, ii) switching losses where the gate capacitance and output capacitance are the main factors of switching loss, and iii) control losses. The control losses analysis is based on the control circuit designed in [38, 39].

To calculate the conduction losses of inductor where the parasitic resistance (R_{ESR}) has a huge impact of power efficiency of DC-DC converter, MOSFET (R_{on}), and the diode, the following expressions can be written as [35, 38, and 39]:

$$P_{conduction} = \alpha * (P_{cond,L} + P_{cond,MOSFET} + P_{cond,diode}) \quad (3.17)$$

$$P_{cond,L} = I_{L,rms}^2 * R_{L,ESR} \quad (3.18)$$

$$P_{cond,MOSFET} = I_{MOSFET,rms}^2 * R_{on} \quad (3.19)$$

$$P_{cond,diode} = \frac{V_F i_{peak} D_1 T_s V_S}{2(V_R - V_S)} \quad (3.20)$$

where the current flowing through the inductor is [24, 38, and 39]

$$I_{L,rms} = i_{peak} \sqrt{\frac{D_1 * V_R}{3(V_R - V_S)}} \quad (3.21)$$

and

$$I_{MOSFET,rms} = i_{peak} \sqrt{\frac{D_1}{3}} \quad (3.22)$$

where

$$i_{peak} = \frac{V_S D_1 T_s}{L} \quad (3.23)$$

The switching loss of MOSFET can be written as

$$P_{switching} = P_{gate\ cap} + P_{gate_drain\ cap} + P_{output\ cap} \quad (3.24)$$

$$P_{gate\ cap} = \frac{Q_g V_S}{2T_s} \quad (3.25)$$

$$P_{gate_drain\ cap} = \frac{Q_{gd} V_S}{2T_s} \quad (3.26)$$

$$P_{output\ cap} = \frac{C_{oss} V_s^2}{2T_s} \quad (3.27)$$

where Q_g , Q_{gd} and C_{oss} are gate capacitance, gate drain capacitance, and output capacitance of MOSFET. The switching power after adding switching factor can be written as

$$P_{switching} = \frac{\alpha}{2T_s} [(Q_g + Q_{gd})V_R + C_{oss} V_s^2] \quad (3.28)$$

Note that switching loss of diode, and other losses are not considered in power loss analysis since they are irrelevant to the converter efficiency and relatively small [35, 38, and 39]. The components of boost DC-DC converter such as MOSFET, inductor, and diode must be chosen carefully in order to minimize the power loss and maximize the converter efficiency and total system efficiency. For example, the equivalent series resistance (R_{ESR}) of inductor is the main factor of conduction loss of the inductor and must have the lowest possible value. This means that the size of inductor will be quite larger. The equivalent series resistance (R_{ESR}) of inductor can be expressed as [38, 39]

$$R_{L,ESR} = (8*10^{12})*L^4 - (1*10^{10})*L^3 + (4*10^6)*L^2 + 3909L \quad (3.29)$$

MOSFET also should some specifications in order to minimize the power loss such as lower R_{on} , lower C_{oss} , and lower Q_g . However, increasing the size of MOSFET leads to lower R_{on} and higher C_{oss} and Q_g . So, a tradeoff between R_{on} and C_{oss} should be considered to achieve reasonable small power loss. The Schottky diode is a better choice since it has lower forward voltage compared to conventional diodes.

3.3.2 Control Circuit

In order to implement the MPPT system using boost DC-DC converter, it is necessary to have a control circuit with a square wave in order to drive/control the gate of the MOSFET. This

control circuit should have the lowest power dissipation to maximize the power efficiency and enhance the power transfer.

The main issue appearing during designing and implementation of a control circuit is how to optimize the values of components that used in DC-DC converter design to make sure that the power efficiency is enhanced compared to conventional MPPT with minimum physical space and without adding more components where the power loss is crucial. Another issue is matching the simulation values of components like the inductance value where these values are the optimum values in terms of power efficiency with the discrete available commercial components in the market. To make a fair comparison, the control circuit design in [38, 39] is used in this work where the gate of MOSFET can be driven using programmable oscillator and comparator as shown in Fig. 3.7. The programmable oscillator generates a square waveform to the gate of MOSFET to turn it on or off based on data coming from the first oscillator. The selection of the control circuit design components (programmable oscillator and power comparator) is not only to maximize the power transfer but also minimize the dissipation power of control circuit.

The control circuit consists of a programmable oscillator (LTC6906) with low supply voltage and range of frequency up to 1 MHz, the frequency can be programmed using this expression [109].

$$F_{out} = \frac{1MHz}{N} \cdot \frac{100k}{R_{set}} = T^{-1}_s \quad (3.30)$$

where N is

$$N = \begin{cases} 10, & DIV\ pin = V^+ \\ 3, & DIV\ pin = open \\ 1 & DIV\ pin = gnd \end{cases} \quad (3.31)$$

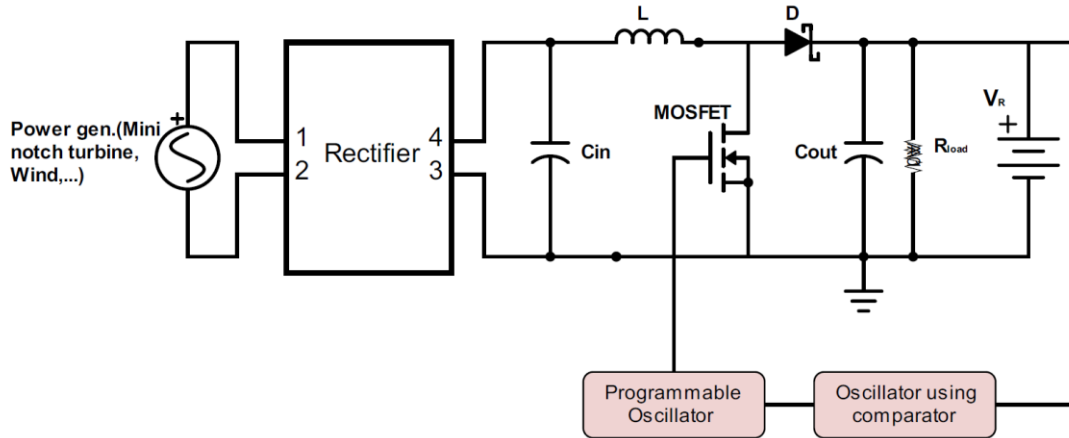


Figure 3.7: MPPT design using programmable oscillator and comparator [38, 39].

3.4 Boost Converter Configuration with PSO Technique

The emphasis in the selection of the optimum values of boost DC-DC converter's parameters in order to match the impedance between energy harvester source and the load parameters (D_1T_s , L , and α) has been executed through an optimization technique called particle swarm optimization computer simulations. As a result, the power efficiency has been increased by 10% compared to previous design without adding any more components. Furthermore, the new enhanced MPPT design reduces the footprint of PCB and physical size of MPPT which is important in low power applications.

3.4.1 Particle Swarm Optimization (PSO) Technique

Particle Swarm Optimization (PSO) finds the best possible solution according to a predefined fitness function for a nonlinear problem by moving interacting particles and choosing the best solutions by comparing the particle's best solution with the global best solution obtained by all particles [111]. This technique was proposed in 1995, based on analogy with biological swarming observed in insect swarms, bird flocks, and fish schools [112]. PSO technique is

capable of achieving solid, accurate, and rapid solutions to several complex optimization problems.

The main idea of PSO is finding the best result or at least acceptable result for a multi-dimensional optimization issue based on the movement of particles and interactions between them by comparing the best personal solution of each particle and the best global one using a known fitness function [111-116]. The aim of applying PSO algorithm is to have best values of L and D_1T_s that can output maximum converter efficiency. The selection of values of the inductor and on time for boost converter depends on power losses, emulated resistance, input power, and output voltage.

Particle swarm optimization (PSO) is a stochastic, adaptive population-based algorithm similar to simulated annealing and genetic algorithm. It's a large number of searches using a group of particles and interactions between them and uses swarm communication and intelligence to achieve the goal of optimizing a problem based on fitness function [114-116].

Particle Swarm Optimization (PSO) finds the best possible solution according to a predefined fitness function for a nonlinear problem by moving interacting particles and choosing the best solutions by comparing the particle's best solution with the global best solution obtained by all particles [111]. PSO technique is capable of achieving solid, accurate, and rapid solutions to several complex optimization problems. The primary idea of PSO is purchasing the best result or at least satisfactory result for a multi-dimensional optimization issue based on the movement of particles and the interactions between them by comparing the best personal solution of each particle and the best global one based on information of fitness function, location, and velocity of particles [112-113].

3.4.1.1 PSO Language for MPPT

1. Particle: is a swarm member (one bee/bird, which represents the configuration of maximum power point circuit design).
2. Swarm: the whole set of particles (bees/birds, which represent the maximum power point circuit designs).
3. Fitness function: the location and velocity of particles will be updated and directed into the global solution based on fitness function, in this research, the fitness function represents the power efficiency.
4. Fitness value: it's a number returned from the fitness function describing how much is the goodness of the solution, the higher fitness value, the better solution. In MPPT design language it means the realistic values of inductor, on time, and switching factor and maximum power efficiency.
5. Pbest: personal best, which is the location of the best solution. It means the location that has the best fitness value (best MPPT design with maximum power efficiency)
6. Gbest: Global best, which is the location of the best solution obtained from all the swarm by comparing all particles' pbests and select it, where the best solution has highest power efficiency (best MPPT configuration).
7. Solution space: represents the field where the particles are allowed to search and it's determined by putting a maximum and minimum realistic limits allowed for the particles to reach [113, 114, and 116].

3.4.1.2 PSO Flow Chart

PSO algorithm follows the steps below:

1. Define the solution space: provide the parameters that need to be optimized a reasonable range in order to search for the optimal solution. Thus means to specify a minimum and maximum weight for each dimension, so particles can't step out to reach out the solution.
2. Define a fitness function: In this work, the fitness function represents the power efficiency expression to evaluate the minimum power loss and maximize the output power coming from MPPT circuit.
3. Initialize random swarm position and velocity of each particle in the D-dimensional problem, the position of particle i is represented as $L_i = [l_{i1}, l_{i2}, \dots, l_{iD}]$, and the velocity of particle i is represented as $V_i = [v_{i1}, v_{i2}, \dots, v_{iD}]$. For a D-dimensional problem, the position and velocity can be represented as [117]

$$L = \begin{pmatrix} l_{11} & \dots & l_{1D} \\ \vdots & \ddots & \vdots \\ l_{N1} & \dots & l_{ND} \end{pmatrix} \quad (3.32)$$

$$V = \begin{pmatrix} v_{11} & \dots & v_{1D} \\ \vdots & \ddots & \vdots \\ v_{N1} & \dots & v_{ND} \end{pmatrix} \quad (3.33)$$

where N is the number of particles in the swarm.

4. Particles movement and direction through solution space. Each particle moving inside the space solution is following these steps:
 - a. Evaluate the solution found by each particle using the boundary conditions, fitness function, and values of parameters to get a fitness value and compare it with the other solutions founded.

- b. Compare the existing solution with the pbest, and if it's better than pbest, then pbest will be substituted by velocity and position of the new solution, and if not, then this solution is discarded.
 - c. Compare the existing solution with the gbest, if the new solution is better than gbest, then gbest will be substituted by velocity and position of the pbest.
 - d. Update the particle's velocity based on PSO expressions
 - e. Update the particle's location based on PSO expressions [114-117]
5. Repeating: the process is repeated for all particles starting step 4, all the positions are evaluated and refined to the position of best/global solutions, this approach produces a global best position vector and personal best position matrix as shown below [117]:

$$P = \begin{pmatrix} P_{11} & \cdots & P_{1D} \\ \vdots & \ddots & \vdots \\ P_{N1} & \cdots & P_{ND} \end{pmatrix} \quad (3.34)$$

$$G = [g_1 \quad g_2 \quad g_3 \quad \cdots \quad g_D] \quad (3.35)$$

6. Repeat step 5 until the maximum iteration is reached, or the target is achieved. Fig. 3.8 summaries the PSO algorithm that used in MPPT design

3.4.1.3 Velocity and Position Updates

Particle velocity in PSO algorithm is updated according to [118-120]:

$$v_{id}^t = w * v_{id}^{t-1} + c_1 * r_{d1}^t * (p_{id}^t - l_{id}^{t-1}) + c_2 * r_{d2}^t * (g_d^t - l_{id}^{t-1}) \quad (3.36)$$

where v_{id}^t is the current velocity of particle i in d^{th} dimension, v_{id}^{t-1} is the previous velocity, l_{id}^{t-1} is the previous position, w is the inertia factor [0,1], c_1, c_2 are user-defined constants, p_{id}^t is the current pbest, g_d^t is the current global solution, and r_{d1}^t, r_{d2}^t random numbers in the range of [0, 1] used to address the variety of the swarm. Particle position is updated according to [118-123]:

$$l_{id}^t = l_{id}^{t-1} + v_{id}^t * \Delta t \quad (3.37)$$

where l_{id}^t is the new position, l_{id}^{t-1} is the previous position, Δt is time step.

3.4.2 PSO Parameters Value Selection

The parameters used in PSO technique are listed in Table 3.1, where each parameter's range is also specified.

3.4.3 Selection of L and D_1T_s

PSO optimization technique is used to find the best value of L and D_1T_s that can produce high converter efficiency by run simulation over expressions (3.17-3.29). The selection of values of inductor and on time for the design of the boost converter depends on power losses, emulated resistance, input power, and output voltage, the following steps should be followed:

Table 3.1: PSO Parameters

Parameter	Range
Δt	1
Inertia weight (w)	0-1
r_1, r_2	0-1
c_1, c_2	2.05
Iteration numbers	1000
Swarm size	49

1. Initialize randomly the positions of the particles by providing each particle one setup of maximum power point tracking system in PSO algorithm. For DC-DC converter with emulation resistor technique:

$$\begin{aligned}
&\text{Particle \#1} : [L_1 D_1 T_s \alpha_1] \\
&\text{Particle \#2} : [L_2 D_1 T_s \alpha_2] \\
&\quad \cdot \\
&\quad \cdot \\
&\quad \cdot \\
&\text{Particle \#n} : [L_n D_n T_s \alpha_n]
\end{aligned} \tag{3.38}$$

2. Initialize the velocity of each particle.
3. Initialize the personal best/global values that can be calculated using fitness function, in this work, the fitness function is:

$$R_{optimum} = \frac{V_s^2}{P_{input}} = \frac{2L}{D_1^2 T_s \alpha} \left(\frac{V_R - V_s}{V_R} \right) \tag{3.39}$$

Boundary conditions are must be considered to maintain the parameters of maximum power point tracking system within the permitted values. Therefore, the following conditions should be satisfied.

1. The inductance of the DC-DC converter should be within practical values and the requirements of the industry.
2. The on-time of the MOSFET should be positive and within practical values.

3.5 Simulation Results

To demonstrate proposed work, the solution space is intended to keep parameter values that are used in optimization within acceptable ranges. Ranges used in this paper are listed in Table 3.2. After these simulations are run at minimum (50μW) and maximum (500μW) input power levels and minimum (50Ω) and maximum (800Ω) emulated resistances, results of applying PSO on expressions (3.17-3.29) are shown in Fig. 3.9, where values of optimized L and $D_1 T_s$ of each trial are taken after 1000 iterations or until the stop criteria is satisfied. It can be seen that the converter efficiency changes over the range of emulated resistances where the

maximum converter efficiency of 90.5% is achieved and 80% is achieved for the lowest value of input power.

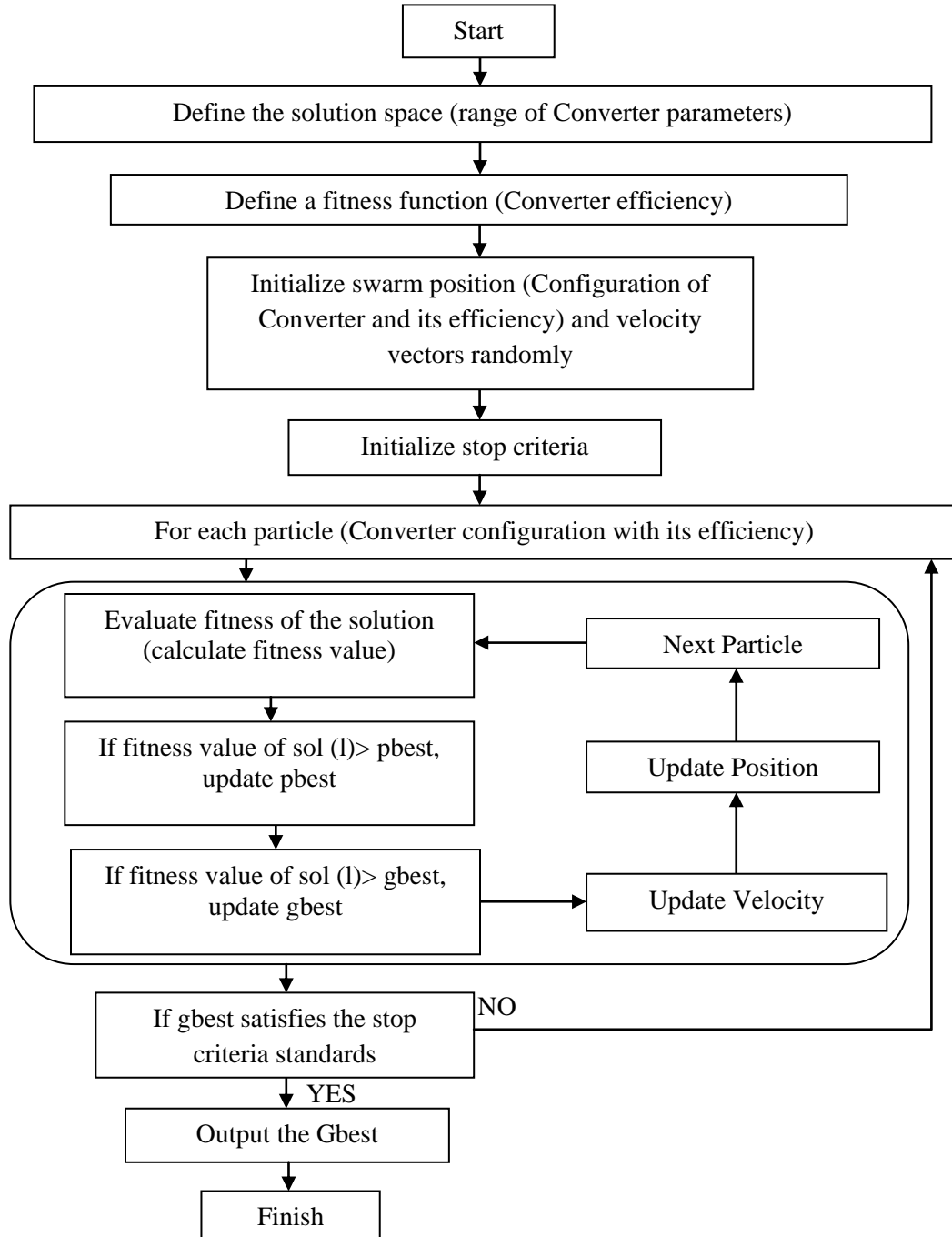


Figure 3.8: Flow chart of PSO presenting MPPT configurations

Fig. 3.10 shows a comparison between PSO simulation results of the optimized MPPT and simulation results of passive MPPT [38, 39] for different values of emulated resistances (200 and 750Ω) over an extended power input range (50 μW-500 μW). It is clear from Fig. 3.10 that converter efficiency using PSO optimization is higher than the converter efficiency of passive MPPT simulation results [38, 39] by almost 9.25% over an extended power input range (50 μW-500 μW) and reaches up to 90.8% for $R_{em}=1000\Omega$. Also, it shows that optimized converter configuration has 3.5% higher efficiency than adaptive MPPT results [24] and gets higher for higher values of emulated resistances.

Table 3.2: PSO Parameters Values Used in Optimization

Parameter	Range
Emulated resistance	15-1500 Ohm
Input power	50-500 μW, 1mW-10mW
Output Voltage	3.2-4.20V
Inductance	10-750μH
On time	5-100μsec
Diode	V _d =230-270mV
MOSFET	R _{on} =0.344Ω, M _g =650pf, C _{oss} =35pf

Another advantage is that the proposed design can be applied for extremely low power sources like photovoltaic, wind power, and mini notched turbine, because the investigated work is valid for the low emulated resistances. Therefore, the design can be applied with power sources with the low load resistance.

The power loss calculations based on optimized selected parameters of DC-DC boost converter are given in Fig. 3.11 which shows a chart of the loss budget of the transistor-diode boost converter with the selected parameter values. The conduction power loss including diode loss, MOSFET loss, and inductor loss caused by equivalent series resistance dominates the total loss due to increasing the current as expected.

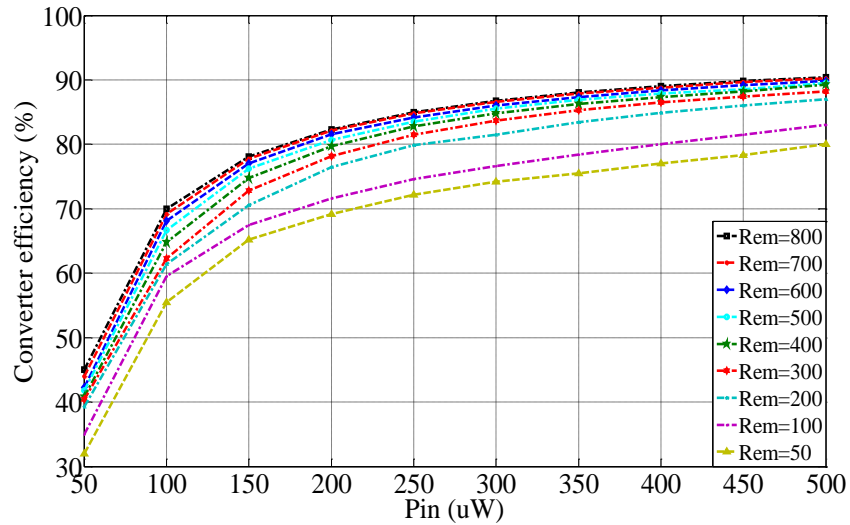


Figure 3.9: Simulation at different values of R_{em} (50-800 Ω) over P_{in} range (50 μ W-500 μ W).

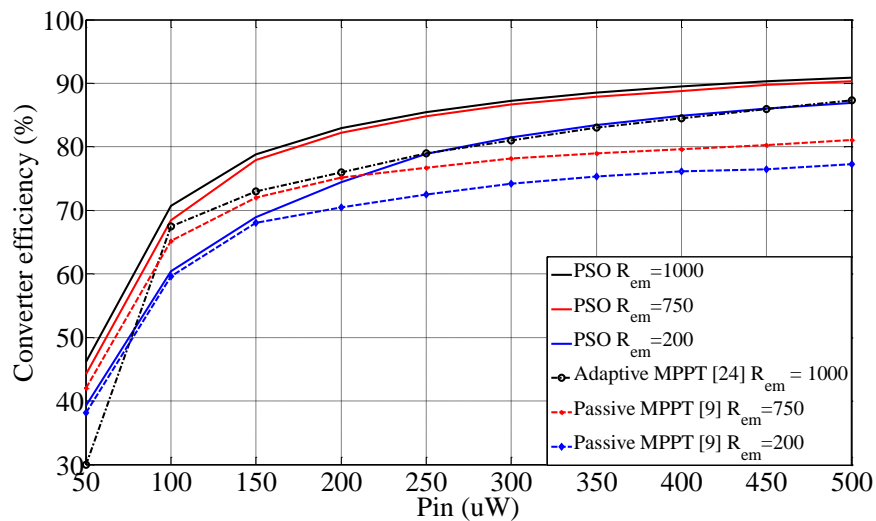


Figure 3.10: PSO simulation results vs. simulation results of passive MPPT [38, 39] of converter efficiency for R_{em} (200 and 750 Ω) and simulation results of adaptive MPPT [24] for $R_{em} = 1000 \Omega$.

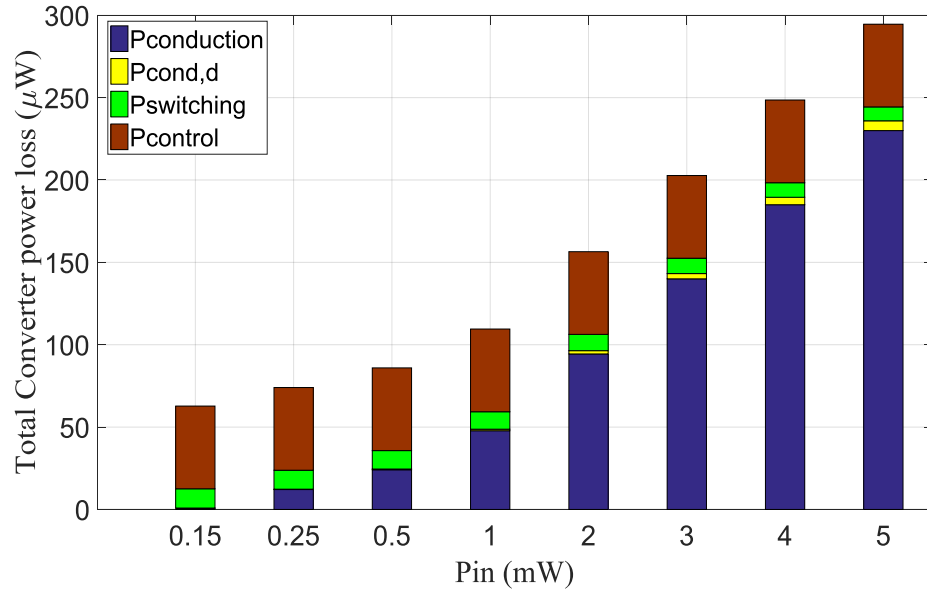


Figure 3.11: Power loss calculations of a DC-DC converter for input power range of (0.15-5mW).

CHAPTER 4:
IMPLEMENTATION OF ENERGY HARVESTING SYSTEM WITH ENHANCED
MAXIMUM POWER TRACKING SYSTEM USING DC-DC BOOST CONVERTER
AND RESISTOR EMULATION

4.1 Introduction

Validation of theory, simulations, concepts, and approaches in the scope of full energy harvesting systems require physical design and implementation of the energy harvester and MPPT system, and measurement results. To demonstrate some of the theory, concepts, and simulations proposed in this research, two energy harvesting systems are fabricated using mini notched turbine and RF rectenna. The goals of this design, implementation, and measurement results will be presented in this chapter. In general, it is possible to demonstrate the theory and concepts with commercial solutions and components which will be faster, inexpensive, and easier. Some of the system components introduced here such as the mini notched turbine or DC-DC boost converter working in the maximum point tracking system requires special design and particular characteristics. Therefore, a full energy harvesting systems will be used in this work to prove the concepts and theory. A novel harvesting mini notched turbine system using fluids for low power devices has been proposed and proven with experimental results. Unlike the conventional turbines, the experimental results of mini notched turbine show that the conversion efficiency increased by 35%. Also, experimental results of proposed enhanced MPPT system show that the power efficiency increased by 7 % compared with previous research without

adding a microcontroller. PSO algorithm is applied in this work to minimize the power loss and enhance the power efficiency of power management circuit by providing the optimum values of DC-DC boost converter.

In Section 4.2, the architecture and implementation of each component of the energy harvesting system (i.e. Mini notched turbine and enhanced MPPT) are presented. Experimental results of mini notched turbine system using proposed enhanced MPPT are given in Section 4.3. The RF rectenna system is built and implemented using enhanced maximum power point tracking system and presented in Section 4.4. The chapter is concluded in Section 4.5.

4.2 Architecture of the Implemented Energy Harvesting System Design

Energy harvesting technology is growing rapidly today regarding low power application and small electronic devices such as smart sensors. As the need for smaller devices and parallel multitasks, energy sources become smaller in size and producing less amount of power. This research and implementation aim to produce a model for enhanced energy harvesting systems with higher capabilities to provide sufficient energy to many low power devices and extend the battery life.

As shown in Fig. 4.1, the energy harvesting system consists of: 1) an energy harvester source, 2) a unique power management circuit placed between energy harvester and load to ensure maximum power transfer, and 3) energy storage/ supercapacitor followed by load which is usually a smart sensor.

4.3 Mini Notched Energy Harvesting System

As was described before in chapter two, the mini notched turbine consists of two parts, the turbine casing and the rotor. It is being prototyped and tested on a miniaturized energy

generator system, which could be used as a green energy source that converts biomechanical energy from some kind of microfluidics to electrical energy.

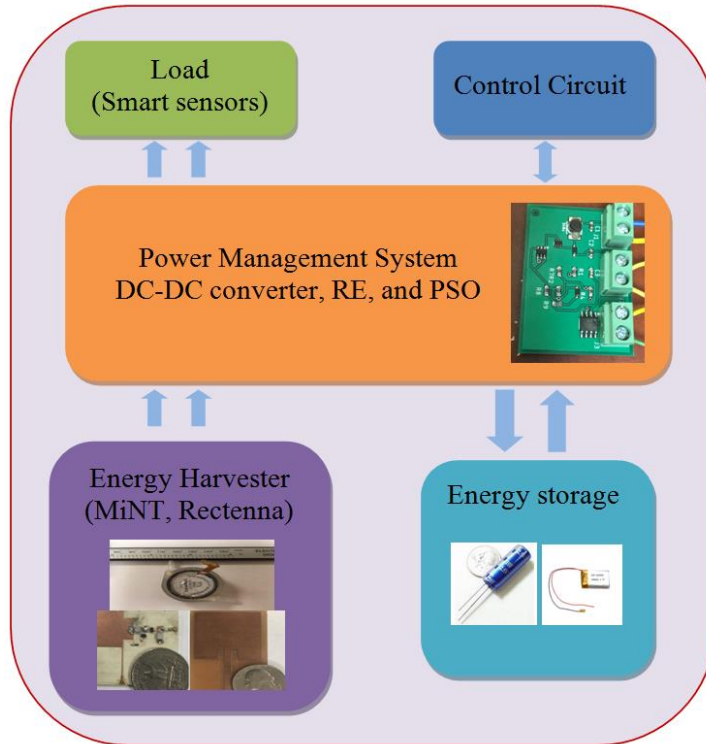


Figure 4.1: Architecture of energy harvesting system design.

The mini notched turbine has increased efficiency over traditional turbine systems because of the changes in the inclination angle of the nozzle and large hub diameter and blade attachment vortices and increasing internal pressure, and because of that, the generated power of the mini notched turbine has been increased by 35% over traditional turbine systems under same conditions [11, 33-35]. The power curves of the mini notched turbine are shown in Fig. 2.7, where these curves are calculated with different resistance loadings to clearly demonstrate the mini notched turbine characteristics. Based on these power curves, the maximum power transfer is obtained when the load resistance is equal to 400Ω . The selection of parameter values for the power management circuit is based on the measured input power levels, input resistance,

optimum resistance, and output power. According to that, a power management circuit is designed and implemented to minimize the power loss and maximize the power transferred to the load.

To better understand the performance and operation of the proposed mini notched turbine system, the circuit configuration of energy harvesting system using MiNT is shown in Fig. 4.2. Based on the power calculations and measurement results of the mini notched turbine system discussed in Section 2.4 and Section 3.4, the mini notched turbine can provide up to 35% increment in output power. The output power could increase the capability of MiNT. Additionally, Enhanced MPPT is able to transfer 7% more power than its other power management system.

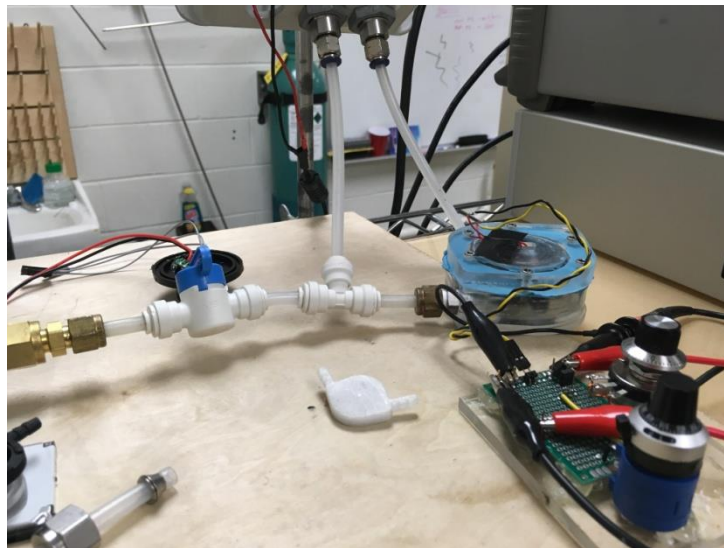


Figure 4.2: Circuit configuration of energy harvesting system using MiNT [12].

As shown in Fig. 4.2, the mini notched turbine energy harvesting system is utilized. A small notched turbine with an overall volume smaller than 15 mm^3 is used as an energy source to harvest and convert power from kinetic energy. The characteristics of the mini notched turbine is obtained experimentally with different loads and different flow rates, followed by the

implementation and design of an enhanced power management system to transfer maximum power obtained by of the MiNT to the load/energy storage.

The mini notched turbine is built in the laboratory using a 3D printer where the cost for fabrication is inexpensive, and a controlled flow meter, pressure sensor, and digital multimeter are used in order to obtain accurate experimental results. The power curves of the mini notched turbine are shown in Fig. 2.7, where these curves are calculated with different resistance loadings to clearly demonstrate the mini notched turbine characteristics. Throughout the experimental procedures of the mini notched turbine, the fluid flow was kept under control using a flow meter controller. Based on power curves in Fig. 2.7, the power management circuit will be designed at optimum resistance equal to input impedance.

4.3.1 Enhanced Power Management Circuit Using DC-DC Converter

In order to harvest and deliver maximum power to the energy storage, a DC-DC converter is implemented in a way that the converter behaves as a matching network to perform maximum power point tracking (MPPT) resistor emulation technique. The enhanced power management system with control circuit is shown in Fig. 4.3.

The control circuit as shown in Fig. 4.3 is used to keep the DC-DC converter operating in discontinuous conduction mode (DCM). The output coming from comparator is used to turn on/off the programmable oscillator in order to provide a waveform for the MOSFET and then maximize the power delivered. PSO optimization technique is used to find the best value of L and D_1T_s that can produce high converter efficiency by run simulation over expressions (3.17-3.29). The selection of values of inductor and on time of MOSFET for the design of the boost converter depends on power losses, emulated resistance, input power, output voltage, PSO parameters.

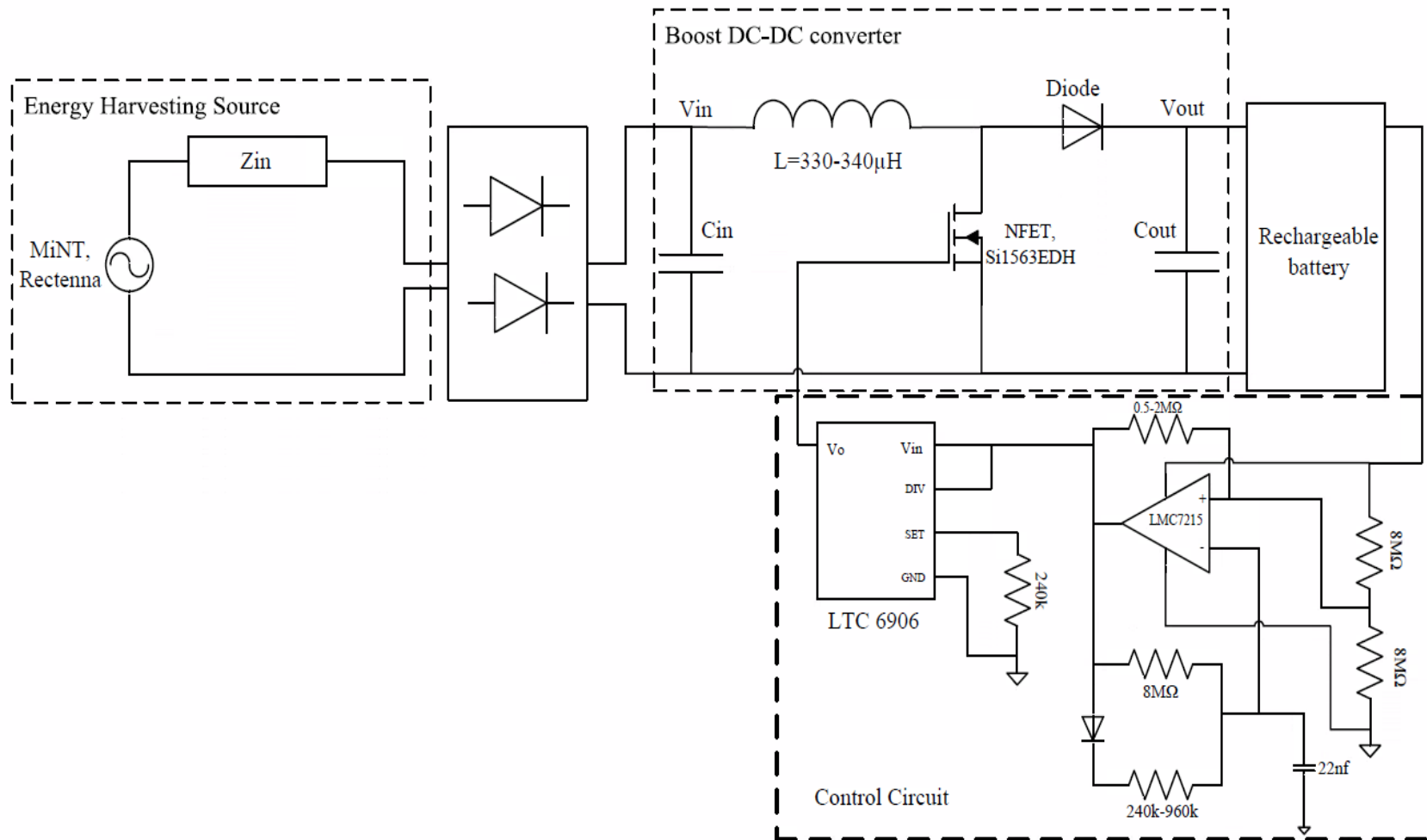


Figure 4.3: Proposed enhanced MPPT

4.3.2 Experimental Results

The mini notched turbine energy harvesting system prototype is implemented and fabricated as shown in Fig. 4.4, as described in Chapter two and Chapter three. Mini notched turbine is used here with internal resistance equal to 400Ω . Thus, the selection of parameters of DC-DC boost converter is optimized based on that.

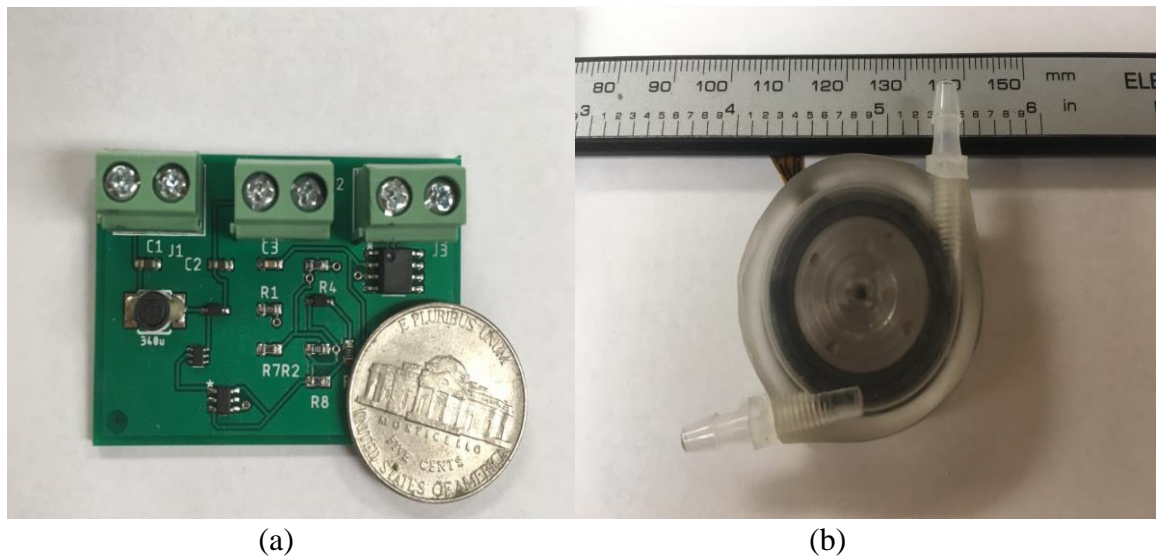


Figure 4.4: Energy harvesting system; a) Enhanced power management system and b) Mini notched turbine [12].

The experiments and power measurements have been performed using some of the laboratory equipment as shown in Fig. 4.5, flow valve controller, oscilloscope, pressure meter, and digital multimeter, and the harvesting system prototype.

The boost DC-DC converter parameters are optimized to ensure minimum power loss and maximum efficiency taking into consideration the availability the optimum values in the market. Consequently, these parameters are selected and boost DC-DC converter is designed using Eagle PCB software.

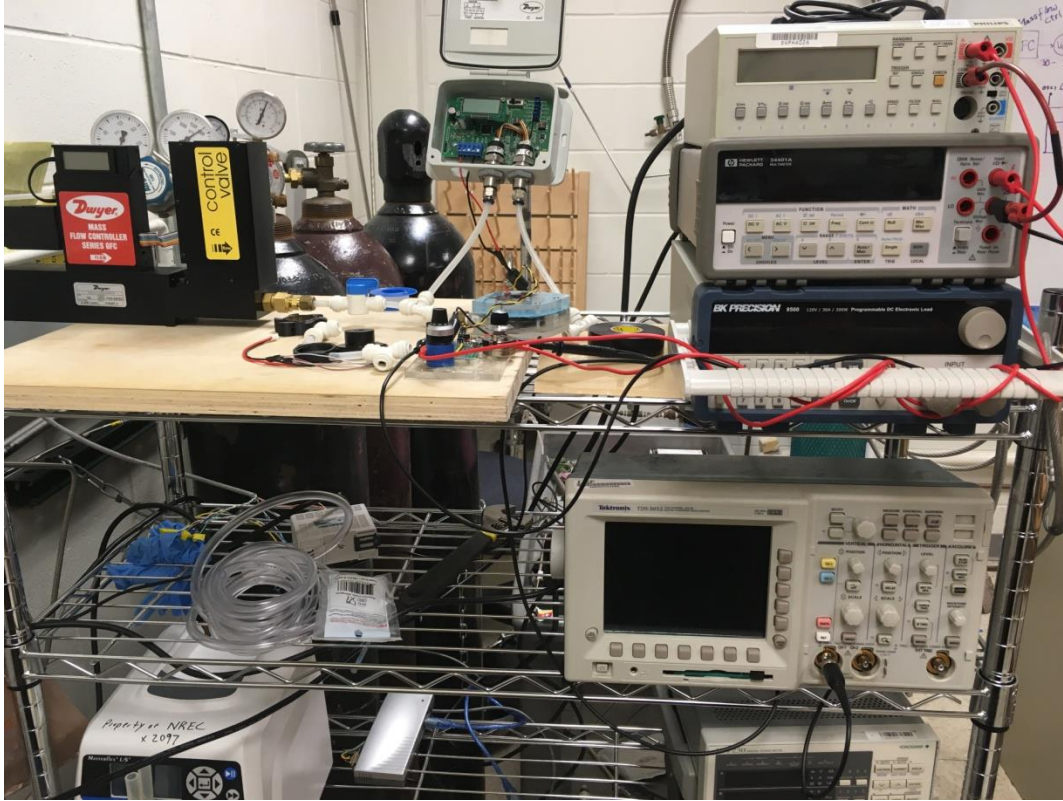


Figure 4.5: The test configuration to measure mini notched turbine energy harvesting performances [12].

The parameters are: $L= 330 \mu\text{H}$, $D_1T_s=12.4\mu\text{s}$, $R_{\text{optimum}} = 400 \Omega$, and input power in the range ($50\mu\text{W}$ - 15mW). To prove experimentally the analysis of resistor emulation using DC-DC boost converter and PSO in order to observe the behavior of enhanced maximum power point tracking (MPPT) for mini notched turbine energy harvesting system. Mini Notched turbine system using enhanced power management circuit has been designed and implemented using some discrete commercial components such as NMOSFET, diodes, and rechargeable lithium thin film battery [124], a 3.9V, 1 mAh, and 160 μm thickness thin film battery from STMicroelectronics. Mini notched turbine is used here with internal resistance equal to 400Ω . Thus, the selection of parameters of DC-DC boost converter is optimized, selected, and designed based on that. The parameters are listed in Table II.

Table 4.1: Enhanced Power Management Circuit Parameters

Parameter	Actual Value
Emulated resistance	400Ohm
Input power	100-500 μ W, 1mW-15mW
Output Voltage	3.9V , thin film battery STMicroelectronics
Inductance	330 μ H
On time	12.4 μ sec
Schottky diode	260mV (BAT43WS)
MOSFET	Si1563EDH (Vishay) $R_{on}=0.344\Omega$, $Q_g=650\text{pf}$, $Q_{gd}=230\text{pf}$ $C_{oss}=35\text{pf}$
Programmable Oscillator	LTC6906, $I_{ss}=12\mu\text{A}$
Comparator	LMC7215, $I_{ss}=0.7\mu\text{A}$
Rectifying Process	260mV (BAT43WS)

A group of experiments were done under controlled environment inside the laboratory. The experimental results of the designed power management circuitry are shown in Fig. 4.6 and Fig. 4.7. Fig. 4.6 and Fig. 4.7 demonstrate that with the proposed power management using PSO and DC-DC converter with resistance emulation technique, more harvested power in the range of (50 μ W-15mW) is transferred and gathered from mini notched turbine system and delivered to the load. Also, the enhanced MPPT has the capability to harvest power and transfer it to the load even with very low input power. Also, Fig. 4.6 and Fig. 4.7 show that the power conversion efficiency is about 85% for 500 μ W input power and reaches 90% for 15mW.

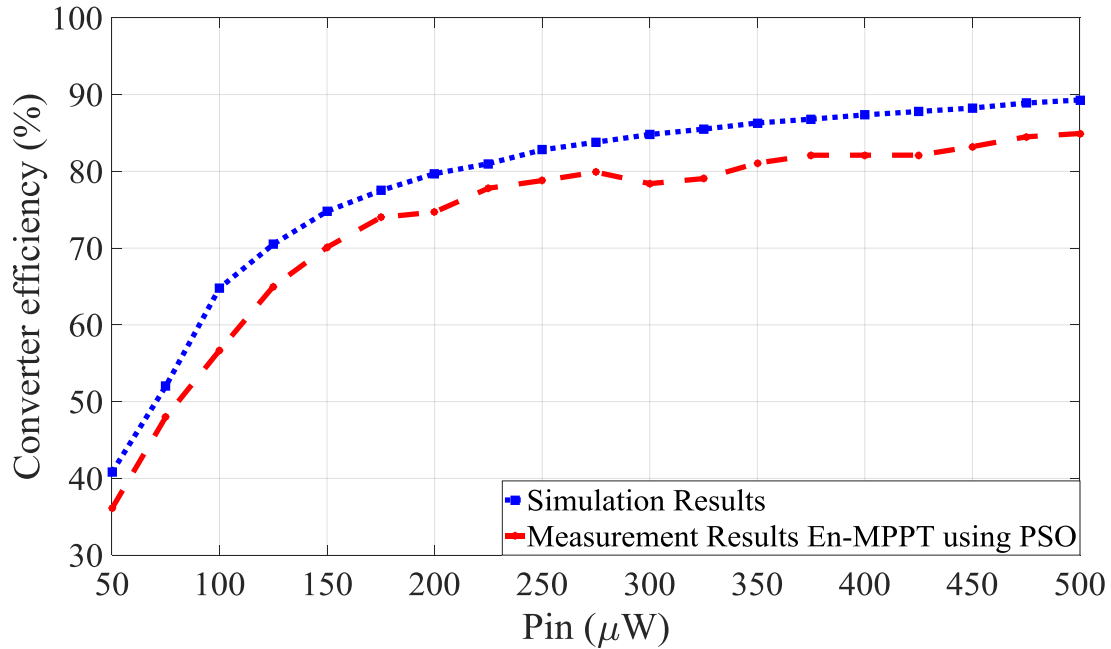


Figure 4.6: Power conversion efficiency of DC-DC boost converter with proposed resistor emulation technique for low input power range.

Close agreement between measurement results obtained experimentally and simulation results is observed in Fig. 4.6 and Fig. 4.7. This agreement verifies the design of proposed enhanced MPPT. Slight difference between measured results and the simulation could be due to tool losses, soldering, or wire losses.

Fig. 4.8 shows a comparison between measurement results of the proposed enhanced MPPT and measurement results from a passive MPPT [38, 39] and active MPPT [24] over an extended low power input range (200 μW -1000 μW). It is clear from Fig. 4.8 that converter power efficiency of enhanced MPPT is higher than the passive MPPT [38, 39] by almost 8% over an extended power input range (200 μW -1000 μW) and reaches up to 87% for $P_{\text{in}}=1000$ μW . These results also show that the optimized converter configuration has 2-3% higher efficiency than adaptive MPPT results [24]. The results indicate more than 8% increasing in power conversion efficiency and harvested power by utilizing the proposed MPPT.

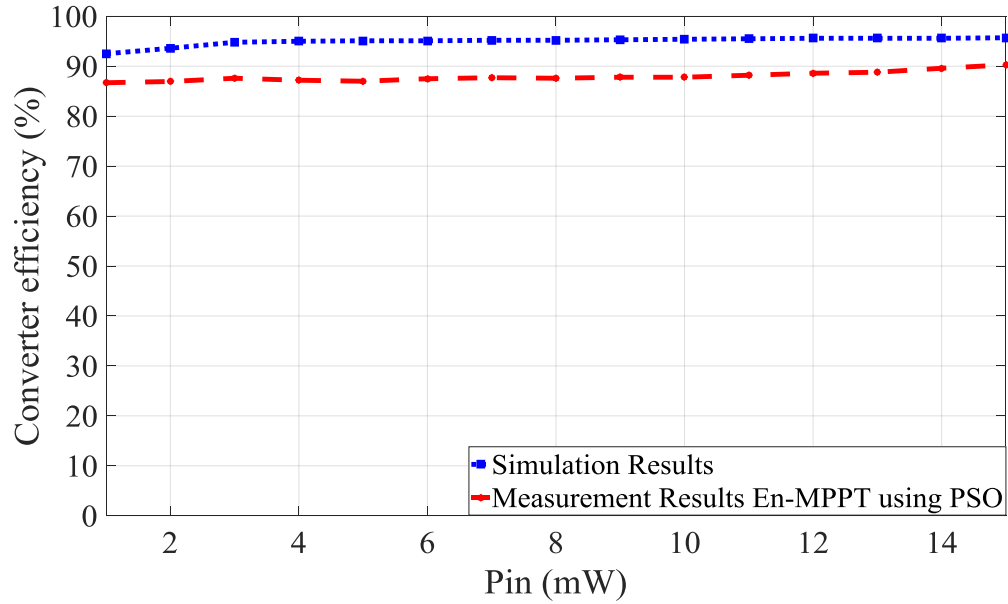


Figure 4.7: Power conversion efficiency of DC-DC boost converter with proposed resistor emulation technique for mild input power range.

Fig. 4.9 shows a comparison between measurement results of the proposed enhanced MPPT and measurement results in [23] and [35] over an extended power input range (1mW-10mW). It is clear from Fig. 4.9 that converter power efficiency of enhanced MPPT is higher than the adaptive MPPT in [23] and [35] by almost 2-4% over an extended power input range and reaches up to 88% for $P_{in}=10$ mW. The results in Fig. 4.9 indicate more than 4% savings in power conversion efficiency by utilizing the proposed Enhanced MPPT technique.

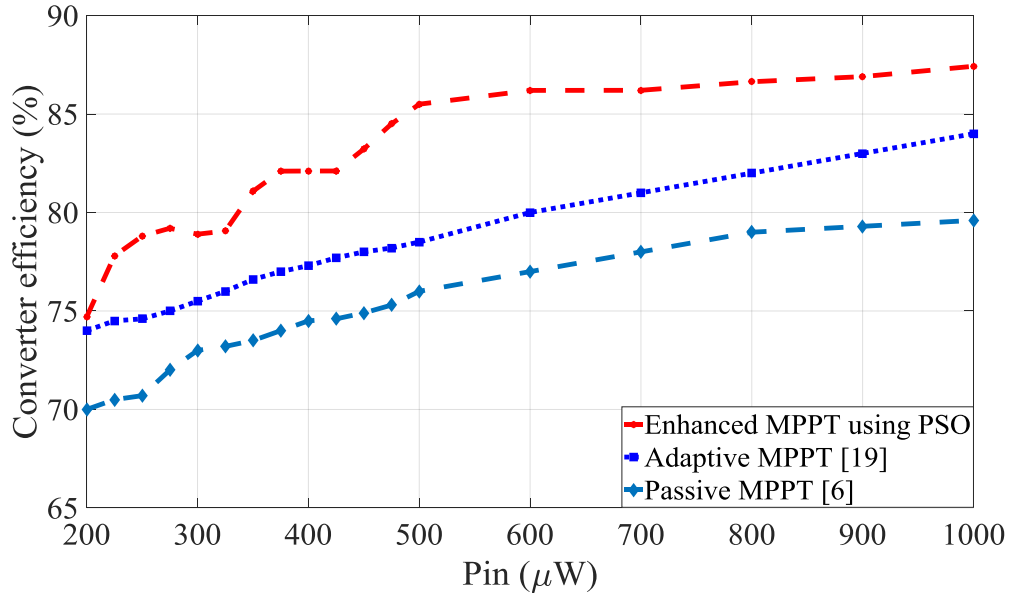


Figure 4.8: Power conversion efficiency comparison in a DC-DC converter over (200 μ -1mW) power input range between the enhanced MPPT and MPPT in [24] and [38, 39]. The power conversion efficiency of DC-DC converter is increased 2-7% by utilizing the proposed MPPT.

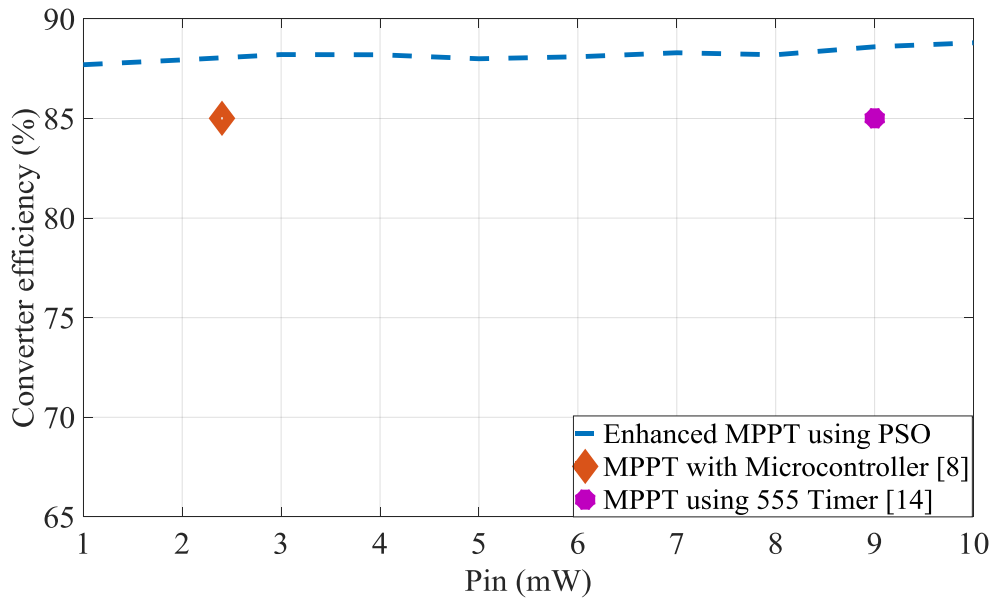


Figure 4.9: Power conversion efficiency comparison in a DC-DC converter over (1mW-10mW) power input range between the enhanced MPPT and MPPT in [23] and [35]. The power conversion efficiency of DC-DC converter is increased 2-3% by utilizing the proposed MPPT.

4.4 RF Rectenna Energy Harvesting System

As was described before in chapter two, the RF rectenna consists of three parts, an antenna, matching network to maximize the power delivered to the load, and a rectifier circuit. It is being fabricated and tested using generator connecting to 2.4 GHz monopole antenna as a power source in order to harvest energy by RF rectenna in Center for Wireless and Microwave Information Systems lab at University of South Florida (WAMI Lab). The power curves of the RF rectenna are shown in Fig. 2.14 where these curves are calculated with different resistance loadings to clearly demonstrate the RF rectenna characteristics. Based on these power curves, the maximum power transfer is obtained when the load resistance is equal to 400 Ω . Based on that, the rectenna was designed and fabricated [125].

The selection of parameter values for the power management circuit is based on the measured input power levels, input resistance, optimum resistance, and output power. According to that, a power management circuit is designed and implemented to minimize the power loss and maximize the power transferred to the load.

To better understand the performance and operation of the RF rectenna energy harvesting system, the circuit configuration of energy harvesting system using rectenna is built and fabricated. Based on the power calculations and measurement results of the RF rectenna system discussed in Section 2.5 and Section 3.4, the power conversion efficiency of rectenna is about 70% (75% simulation).

4.4.1 Experimental Results

The RF rectenna energy harvesting system prototype is implemented and fabricated as shown in Fig. 4.10 as described in Chapter two and Chapter three. RF rectenna is used in this

work where the source internal resistance equal to 400Ω . Thus, the selection of parameters of matching network of RF rectenna and boost DC-DC converter is optimized based on that.

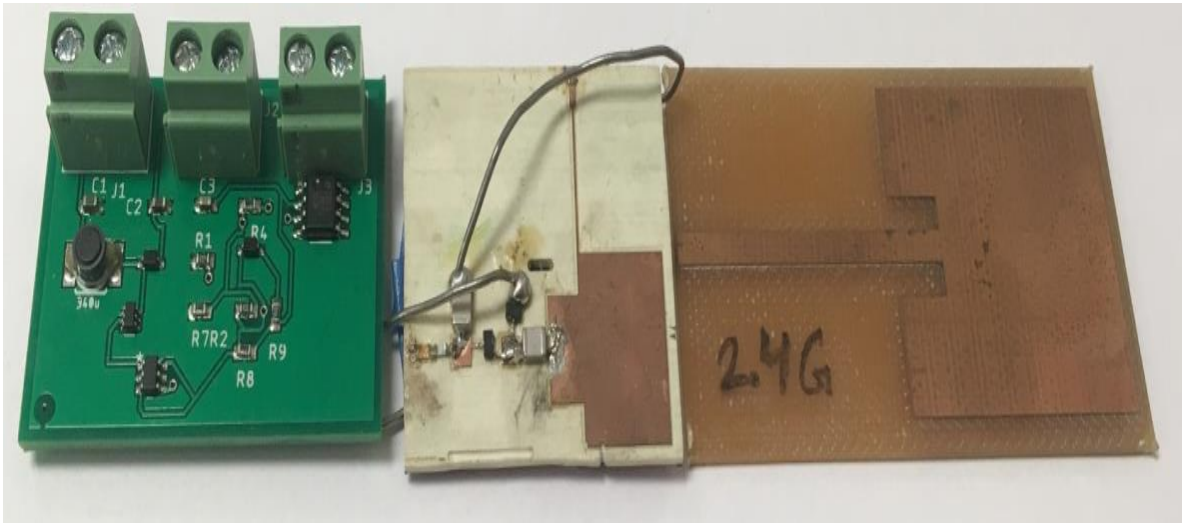


Figure 4.10: RF rectenna energy harvesting system with enhanced MPPT.

As shown in Fig. 2.13, The RF rectenna energy harvesting system is utilized, a small patch antenna with a matching network with rectifier circuit are used as an energy source to harvest energy. The characteristic of the RF rectenna is obtained experimentally with different loads and different input power coming to antenna, followed by the implementation and design of enhanced power management system to transfer maximum power obtained by the energy source to the load/energy storage.

Since the input impedance of mini notched turbine and RF rectenna are equal, the enhanced MPPT that used in mini notched turbine measurement is used again in RF rectenna measurement with same the selection of parameters values. Therefore, a DC-DC converter is implemented in a way that the converter behaves as a second matching network to perform maximum power point tracking (MPPT) resistor emulation technique. The enhanced power management system with the control circuit is shown in Fig. 4.10.

Fig. 4.11 and Fig. 4.12 demonstrate that with the proposed power management using PSO and DC-DC converter with resistance emulation technique, more harvested power in the range of (1mW-20mW) is transferred and gathered from RF rectenna system and delivered to the load. Also, the enhanced MPPT has the capability to harvest power and transfer it to the load even with very low input power. Also, Fig. 4.11 and Fig. 4.12 show that the power conversion efficiency is about 86% for 1mW input power and reaches 91% for 20mW.

Close agreement between measurement results obtained experimentally and simulation results is observed in Fig. 4.11 and Fig. 4.12, this agreement verifies the design of proposed enhanced MPPT, the differences between both measurement results and the simulation ones could be due to the tool losses, soldering, and wires losses.

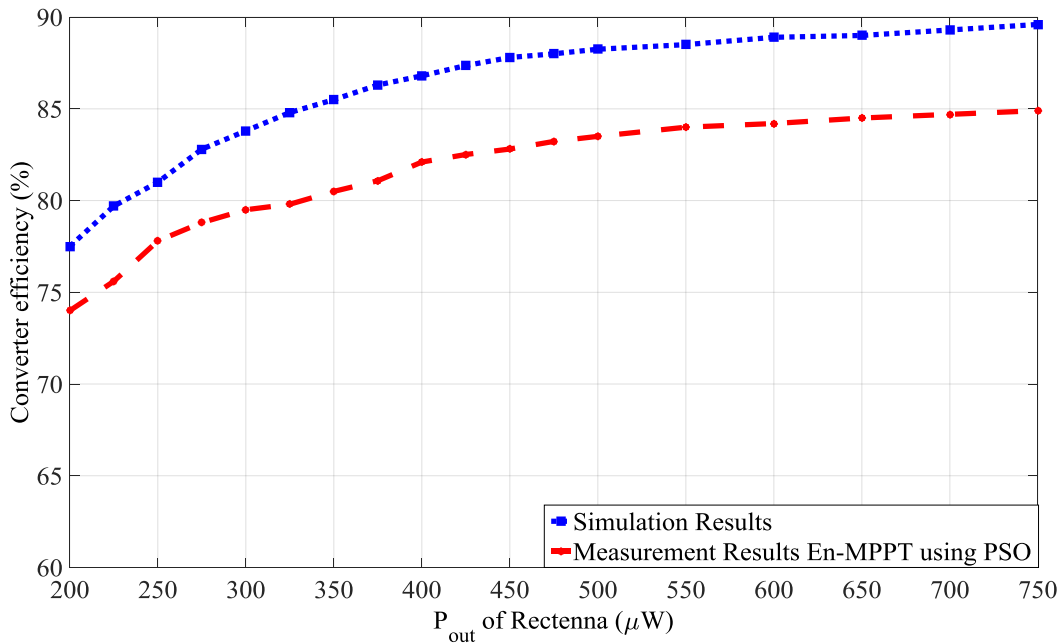


Figure 4.11: Power conversion efficiency of DC-DC boost converter with proposed resistor emulation technique for low input power range coming from RF rectenna.

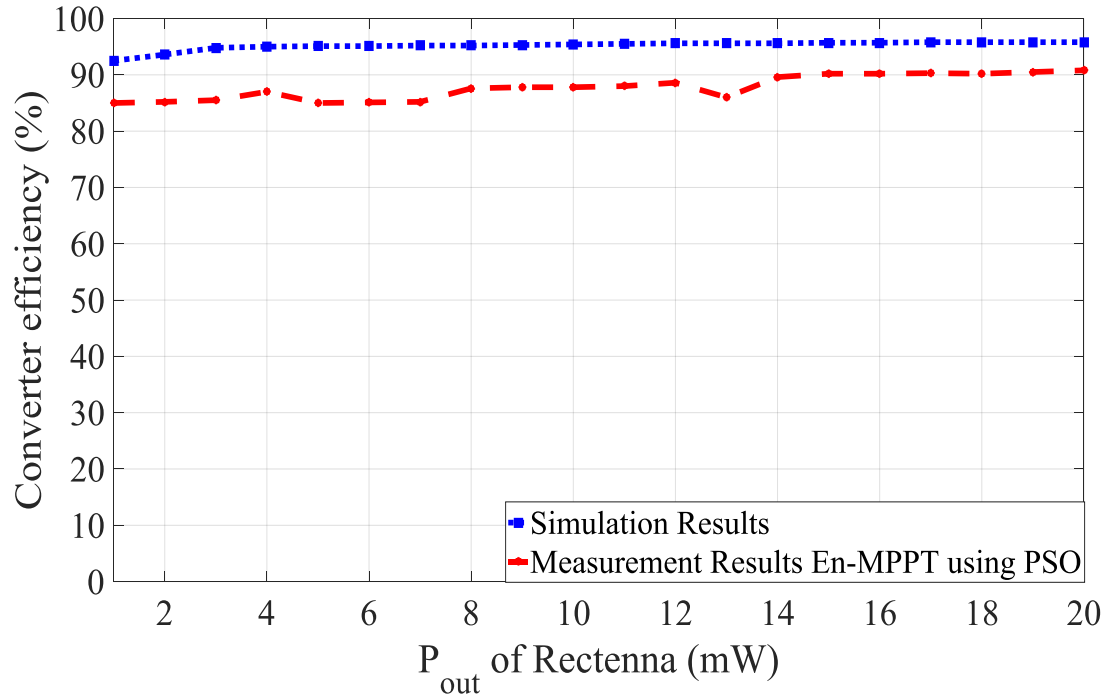


Figure 4.12: Power conversion efficiency of DC-DC boost converter with proposed resistor emulation technique for input power range coming from RF rectenna.

Enhanced power management circuit differs from other power management models in two main ways. First, the power efficiency of the converter has been improved by 7% for low range power input. Second, the PCB footprint of enhanced power management circuit has been reduced compared to previous models where is no need for microcontroller since it has high power loss and the size of a microcontroller is relatively large compared to other components that used in the design. Adding a microcontroller with sensing circuit to sense the maximum power point will improve the power efficiency but will increase the PCB footprint significantly. However, the power efficiency of enhanced power management circuit is improved significantly without adding any extra components. Furthermore, the PCB footprint is reduced. Third, the enhanced power management circuit has the capability to be used in different energy sources, different applications and for high power range.

4.5 Mini Notched Turbine Vs. RF Rectenna

Based on the measurement results of the enhanced power point tracking system based on resistor emulation and particle swarm optimization, the enhanced MPPT shows almost same persistence in the converter efficiency behavior over a wide range of input power. Accordingly, the proposed enhanced MPPT can be advantageous for most of energy harvesting sources such as solar cell, wind turbines, and piezoelectric.

Result differences between mini notched turbine and RF rectenna will be dependent upon the size, fabricated material, input power, source of energy and application. Both the mini notched turbine and RF rectenna could be used *in vivo* applications to deliver power to smart monitoring sensors such as for a glucose sensor where the mini notched turbine output depends on the blood flow and RF rectenna depends on electromagnetic waves. Overall, this innovative power management system has been proven viable for two energy sources, mini notched turbine and RF rectenna, and can be applicable for various other energy sources which may be dependent on the availability of fluid flow or electromagnetic waves, amount of power needed, and the application.

CHAPTER 5:

CONCLUSIONS AND FUTURE WORK

An understanding of how energy harvesting systems work is provided in this work, and moreover, this work concentrates on delivering and improving the power efficiency of a power management system used for the novel MiNT technology and other energy harvesting systems. Two fully integrated energy harvesting systems are designed, built, and tested as the final target of this work. More power harvested, less physical size, increased reliability, and improved converter power efficiency are accomplished compared to conventional energy harvesting systems.

In summary, the following contributions to the field of power electronics for low power systems has been accomplished: i) enhanced power management of the power generated by the novel mini notched turbine technology, ii) expanded the capability of using the mini notched turbine as a sustainable energy harvesting source for low power applications by developing a IC to support the technology, iii) provided a tested technique to improve the power efficiency of enhanced power management systems by using boost converter with resistor emulation technique and particle swarm optimization compared to conventional power management systems, and iv) demonstrated that an enhanced MPPT can be applicable to most low power energy harvesting sources such as solar cell, wind turbines, and piezoelectric.

A novel mini notched turbine that can be used as a feasible energy source to meet the power requirements of small embedded systems is presented in Chapter 2. A novel mini notched

turbine harvester is introduced with an overall volume smaller than 15 mm^3 . Mini notched turbine is being prototyped and tested on a miniaturized energy generator system, which could be used as a green energy source that converts biomechanical energy from some kinds of microfluidics to electrical energy. The design of this novel turbine is developed with environmental and biomedical applications [6-8, 19], in mind. Materials, size, and the assembling of parts are critical issues in design and final assembly of prototypes. In addition, bio-systems could be developed, if the system is built with biocompatible materials, transforming it into a bio micro turbine with the possibility to be used in medical devices as part of a system implanted on a living organism. The generated power of the mini notched turbine has been increased by 35% over traditional turbine systems under same conditions.

An RF rectenna that can be used as a feasible energy source to meet the power requirements of small embedded systems is presented in Chapter 2. RF rectenna is being prototyped and tested on a miniaturized energy generator system, which could be used as a green energy source using a matching network to ensure maximum power transfer and rectifier to convert the energy in useful DC power to use it later for low power devices. Results demonstrate that the maximum converter efficiency of rectenna design is 70% for optimum $R_L=400\Omega$. In order to harvest the maximum power from any energy harvesting source, power management system is needed. However, most of the power management systems are not efficient due to power consumption in control circuitry. Chapter 3 presents an approach for gathering near maximum power by improving the efficiency of DC-DC converter. Convenient power management circuits are not suitable for very low power energy sources due to the high power consumption of components that used in the system. Based on that, particle swarm optimization (PSO) technique is successfully applied to select proper values of inductor and on-time to

minimize power consumption, improve DC-DC converter efficiency, and the efficiency of power management system where the converter efficiency is used as fitness function and inductor and on-time are chosen as optimized parameters [35, 38, 39, 126-130]. This new design improves the efficiency of optimized power management circuit up to 7% compared to conventional power management circuits over a wide range of input power and range of emulated resistances, allowing harvesting more power from small energy harvesting sources and delivering it to the load such as smart sensors. Another advantage is that the proposed approach can be applied for extremely low energy sources and because of that the proposed work is valid for low emulated resistances. Therefore it can be applied with any energy sources with the low load resistance.

To prove and verify the analysis and simulation results, two renewable energy harvesting systems with proposed enhanced power management circuit are designed and built in Chapter 4. The emphasis of circuit design concentrates on improving the power efficiency using proposed enhanced MPPT method presented in Chapter 3. The optimized parameters of the design are: $L=330\ \mu\text{H}$, $D_1T_s=12\ \mu\text{s}$, $R_{\text{optimum}} = 400\ \Omega$, and input power in the range (50 μW -15mW). The measurement results shown in Chapter 4 demonstrate that the optimized DC-DC converter configuration has 2-7% higher power conversion efficiency than conventional power management system.

Finally, the main objectives mentioned in this work have been tested and accomplished. Some of this research has been published already in IEEE conferences inside USA, international IEEE conferences, and journals, and the rest of this research will be submitted to top-tier IEEE journals.

5.1 Future Work

The research work introduced in this dissertation has the potential for many exciting applications such as smart sensor applications, implanted biomedical devices, and ultra-low power applications by providing solutions in places where energy sources are limited. Miniaturization of mini notched turbine energy system and RF rectenna would help both systems to be used as a feasible source for implantable medical devices. This could provide unlimited energy for the lifespan of implanted devices. Since the rectenna could be a potential energy source used for biomedical devices, the material used in antenna designs could be biocompatible materials such as Silicon Carbide (SiC) or antennas coated with biocompatible materials. A 4H-SiC semi-insulating substrate is an ideal substrate for the RF rectenna because it has no microwave signal loss and thus possibly yielding the maximum possible antenna efficiency. A high dielectric constant ($\epsilon_r \sim 10$) semi-insulating 4H-SiC semiconductor substrate could be used later for future work.

The analysis of enhanced MPPT presented in Chapter 3, provides the flexibility to apply it to different DC-DC converters such as buck and buck-boost converters where the fitness function is the main expression used in particle swarm optimization.

Further research of energy harvesting circuits could be towards flexible printed circuit boards where power management circuitry and smart sensors could be integrated on/under the energy harvesting source. This process could reduce the PCB foot print and reduce the physical size of the energy harvesting system

REFERENCES

- [1] D. C. Leslie, *et al*, “A bioinspired omniphobic surface coating on medical devices prevents thrombosis and biofouling,” *Nat. Biotechnol.*, Vol. 32, No. 11, pp. 1134–1140, Nov. 2014.
- [2] S. Roundy, P. Wright, J. Rabaey, *Energy Scavenging for Wireless Sensor Networks*, Kluwer Academic Publishers, Boston MA, 2004.
- [3] D.J. Cook and S.K. Das, “Wireless Sensor Networks”, *Smart Environments: Technologies, Protocols and Applications*, John Wiley, New York, 2004
- [4] J. P. Thomas, M. A. Qidwai, and J. C. Kellogg, “Energy scavenging for small scale unmanned systems,” *Journal of Power Sources*, Vol.159, pp.1494-1509, 2006.
- [5] J.A. Paradiso, T. Starner, “Energy scavenging for mobile and wireless electronics,” *IEEE Pervasive Computing*, Vol.4, Issue 1, pp.18-27, 2005.
- [6] K. Bazaka and M. V. Jacob, “Implantable Devices: Issues and Challenges,” *Electronics*, Vol. 2, No. 1, pp. 1–34, 2012.
- [7] J. Martinez-Quijada and S. Chowdhury, “A two-stator MEMS power generator for cardiac pacemakers,” *IEEE International Symposium on Circuits and Systems, 2008. ISCAS 2008*, 2008, pp. 161–164
- [8] J. Martinez-Quijada and S. Chowdhury, “Body-Motion Driven MEMS Generator for Implantable Biomedical Devices,” *Electrical and Computer Engineering, 2007. CCECE 2007. Canadian Conference on*, 2007, pp. 164–167.
- [9] J. Kymissis, C. Kendall, J. Paradiso, and N. Gershenfeld, “Parasitic power harvesting in shoes,” in *Second International Symposium on Wearable Computers, 1998. Digest of Papers*, 1998, pp. 132–139.
- [10] S. R. Platt, S. Farritor, K. Garvin, and H. Haider, “The use of piezoelectric ceramics for electric power generation within orthopedic implants,” *IEEEASME Trans. Mechatron.*, Vol. 10, No. 4, pp. 455–461, Aug. 2005.
- [11] Henry Cabra,” Design, Simulation, Prototype, and Testing of a Notched Blade Energy Generation System,” Ph.D Thesis, 2014.

- [12] Samuel Perez, "Integration and cross-coupling of a Notched-Turbine Symbiotic Power Source for Implantable Medical Devices," Ph.D Thesis, 2018.
- [13] K. Goto, T. Nakagawa, O. Nakamura, and S. Kawata, "An implantable power supply with an optically rechargeable lithium battery," *Biomed. Eng. IEEE Trans. On*, Vol. 48, No. 7, pp. 830–833, 2001.
- [14] Y. Zhu, S. O. R. Moheimani, and M. R. Yuce, "Ultrasonic Energy Transmission and Conversion Using a 2-D MEMS Resonator," *IEEE Electron Device Letter*, Vol. 31, No. 4, pp. 374–376, Apr. 2010.
- [15] Bert Lenaerts and Robert Puers, "An inductive power link for a wireless endoscope," *Biosens. Electron.*, No. 22, pp. 1390–1395, 2007.
- [16] B. Pless and J. A. Connor, Implantable Power Generator, 2008020096321-Aug-2008.
- [17] P. C.-P. Chao, C. I. Shao, C. X. Lu, and C. K. Sung, "A new energy harvest system with a hula-hoop transformer, micro-generator and interface energy-harvesting circuit," *Microsyst. Technol.*, Vol. 17, No. 5–7, pp. 1025–1036, Jun. 2011.
- [18] Y. D. Choi, J. I. Lim, Y. T. Kim, and Y. H. Lee, "Performance and Internal Flow Characteristics of a Cross-Flow Hydro Turbine by the Shapes of Nozzle and inner Blade," *Journal of Fluid Science and Technology*, Vol. 3, No. 3, pp. 398–409, 2008
- [19] Majdi M. Ababneh, Samuel Perez, Henry Cabra, and Sylvia Thomas, "Design of A Novel Mini Notched Turbine With Optimized Power Management Circuit," *The 8th international Renewable Energy Congress*, March 2017
- [20] Lorentz F. Barstad, "CFD Analysis of a Pelton Turbine," *Norwegian University of Science and Technology, Department of Energy and Process Engineering*, 2012.
- [21] A. Perrig, "Hydrodynamics of the free surface flow in Pelton turbine buckets," *EPFL These*, No. 3715, 2007
- [22] Y. Nakanishi, S. Iio, Y. Takahashi, A. Kato, and T. Ikeda, "Development of a Simple Impulse Turbine for Nano Hydropower," *J. Fluid Sci. Technol.*, Vol. 4, No. 3, pp.567–577, 2009.
- [23] Y. K. Tan, and S. K. Panda, "Optimized Wind Energy Harvesting System Using Resistance Emulator and Active Rectifier for Wireless Sensor Nodes," *IEEE Transactions on Power Electronics*, January 2011, Vol. 26, No. 1, pp. 38-50.
- [24] A. Dolgov, R. Zane, and Z. Popovic, "Power management system for on-line low power RF energy harvesting optimization," *IEEE Trans. Circuits Syst. I*, Vol. 57, No. 7, pp. 1802–1811, Jul. 2010.

- [25] J. D. Jackson and R. F. Fox, ‘Classical electrodynamics,’ *Am. J. Phys.*, Vol. 67, p.841, 1999.
- [26] M. F. Iskander, *Electromagnetic fields and waves*, Prentice Hall Englewood Cliffs, 1992.
- [27] A. Kovetz, *Electromagnetic theory*, Oxford University Press Oxford, 2000.
- [28] Lorentz, F, Barstad, ‘CFD Analysis of a Pelton Turbine,’ Norwegian University of Science and Technology, Department of Energy and Process Engineering, 2012.
- [29] ‘Cross Flow Turbine Design,’
[Online]. Available: <http://www.scribd.com/doc/117792063/CrossFlow-Turbine-Design>.
[Accessed: Mar-2017].
- [30] J.-C. Marongiu, F. Leboeuf, J. Caro, and E. Parkinson, ‘Free surface flows simulations in Pelton turbines using a hybrid SPH-ALE method,’ *J. Hydraul. Res.*, Vol. 48, No. sup1, pp. 40–49, 2010.
- [31] A. Perrig, ‘Hydrodynamics of the free surface flow in Pelton turbine buckets,’ *EPFL These*, No. 3715, 2007.
- [32] B. R. Cobb and K. V. Sharp, ‘Impulse (Turgo and Pelton) turbine performance characteristics and their impact on pico-hydro installations,’ *Renew. Energy*, Vol. 50, pp. 959–964, Feb. 2013.
- [33] H. Cabra and S. W. Thomas, ‘Fabrication of cross flow bio microturbine,’ http://cap.ee.imperial.ac.uk/~pdm97/powermems/2010/posterpdfs/183_Cabra_158.pdf
- [34] Henry Cabra and S. Thomas, ‘Design, Simulation and Prototyping Model of a Miniaturized Bio Energy Generation System,’ *Technical Proceeding of the 22nd IASTED International Symposia on Modeling and Simulation*, MS, 2011.
- [35] Davide Carli, Davide Brunelli, Davide Bertozzi, and Luca Benini, ‘A High-Efficiency Wind-Flow Energy Harvester Using Micro Turbine’. In: *Proc. 20th International Symposium on Power Electronics, Electrical Drives, Automation and Motion (SPEEDAM 2010)*. June 2010, pp. 778–783.
- [36] Majdi M. Ababneh, Samuel Perez, and Sylvia Thomas, ‘Optimized Mini Notched Turbine Energy Harvesting Using Resistor Emulation Approach and Particle Swarm Optimization,’ in *IEEE. SoutheastCon*, March 2017
- [37] Majdi M. Ababneh, Samuel Perez, and Sylvia Thomas, ‘Optimized Power Management Circuit for Implantable Rectenna for In-Body Medical Devices,’ *The 12th IEEE international conference on Power Electronics and Drive Systems*, December 2017
- [38] T. Paing, J. Shin, R. Zane, and Z. Popovic, ‘Resistor Emulation Approach to Low-Power F Energy Harvesting,’ *IEEE Transactions on Power Electronics*, Vol. 23, No. 3, pp. 1494-1501, May 2008.

- [39] T. S. Paing and R. A. Zane, "Resistor emulation approach to low- power energy harvesting," Proc. *IEEE 37th Power Electron. Spec. Conference*, Jeju, S. Korea, pp. 1-7, Jun. 18-22, 2006.
- [40] C. Liu, Y. X. Guo, H. Sun, and S. Xiao, "Design and safety considerations of an implantable rectenna for far-field wireless power transfer," *IEEE Trans. Antennas Propag.*, Vol. 62, No. 11, pp. 5798–5806, Nov. 2014
- [41] P.S. Hall and Y. Hao, *Antennas and Propagation for Body-Centric Wireless Communications*. Norwood, MA, USA: Artech House, 2006.
- [42] A. Kiourti and K. S. Nikita, "A review of implantable patch antennas for biomedical telemetry: Challenges and solutions," *IEEE Antennas Propag. Mag.*, Vol. 54, No. 3, pp. 210–228, Jun. 2012.
- [43] J. Kim and Y. Rahmat-Samii, "Implanted antennas inside a human body: Simulations, designs, and characterizations," *IEEE Trans. Microw. Theory Tech.*, Vol. 52, No. 8, pp. 1934–1943, Aug. 2004
- [44] P. Soontornpipit, C. M. Furse, and Y. C. Chung, "Design of implantable microstrip antennas for communication with medical implants," *IEEE Trans. Microw. Theory Tech.*, vol. 52, no. 8, pp. 1944–1951, Aug. 2004
- [45] Dai and D. C. Ludois, "A survey of wireless power transfer and a critical comparison of inductive and capacitive coupling for small gap applications," *IEEE Trans. Power Electron.*, vol. 30, no. 11, pp. 6017–6029, Nov 2015.
- [46] P. Dular, C. Geuzaine, and W. Legros, "A natural method for coupling magnetodynamic h-formulations and circuit equations," *IEEE Trans. Magn.* , vol. 35, no. 3, pp. 1626–1629, May 1999.
- [47] S. Yoshida, N. Hasegawa, and S. Kawasaki, "Experimental demonstration of microwave power transmission and wireless communication within a prototype reusable spacecraft," *IEEE Microw. Wireless Compon. Lett.* , vol. 25, no. 8, pp. 556–558, Aug. 2015
- [48] N. Shinohara, "Power without wires," *IEEE Microw. Mag.*, vol. 12, no. 7, pp. S64–S73, Dec. 2011.
- [49] "Dengyo rectennas," Nihon Dengyo Kosaku Company Ltd., Tokyo, Japan, Jul. 2012. [Online]. Available: <http://www.den-gyo.com/solution/solution01.html>
- [50] J. Y. Park, S. M. Han, and T. Itoh, "A rectenna design with harmonic rejecting circular-sector antenna," *IEEE Antennas Wireless Propag. Lett.* , vol. 3, pp. 52–54, 2004.

- [51] V. Marian, B. Allard, C. Voltaire, and J. Verdier, "Strategy for microwave energy harvesting from ambient field or a feeding source," *IEEE Trans. Power Electron.*, vol. 27, no. 11, pp. 4481–4491, Nov. 2012.
- [52] M. Pinuela, P. D. Mitcheson, and S. Lucyszyn, "Ambient RF energy harvesting in urban and semi-urban environments," *IEEE Trans. Microw. Theory Techn.*, vol. 61, no. 7, pp. 2715–2726, Jul. 2013.
- [53] S. A. Bhalerao, A. V. Chaudhary, R. B. Deshmukh, R. M. Patrikar, "Powering Wireless Sensor Nodes using Ambient RF Energy," in *Proc. IEEE Int. Conf. on Sys., Man., and Cybernetics*, Taipei, Taiwan, Oct. 2006, vol. 4, pp. 2695-2700.
- [54] U. Olgun, C. C. Chen, J. L. Volakis, "Investigation of Rectenna Array Configurations for Enhanced RF Power Harvesting," *IEEE Antennas and Wireless Propagation Letters*, vol. 10, pp. 262-265, Apr. 2011.
- [55] J. A. Hagerty, Z. B. Popovic, "An experimental and theoretical characterization of a broadband arbitrarily polarized rectenna array," *IEEE MTT-S Int. Micro. Symp. Digest*, Phoenix, AZ, May 2001, pp. 1855-1858.
- [56] C. Walsh, S. Rondineau, M. Jankovic, G. Zhao, Z. A. Popovic, "Conformal 10 GHz rectenna for wireless powering of piezoelectric sensor electronics," in *Proc. IEEE MTT-S Int. Micro. Symp.*, Long Beach, CA, pp. 1-4, Jun. 2005.
- [57] J. A. Hagerty, F. B. Helmbrecht, W. H. McCalpin, R. A. Zane, Z. B. Popovic, "Recycling ambient microwave energy with broad-band rectenna arrays," *IEEE Trans. on Micro. Theo. and Tech.*, vol. 52, no. 3, pp. 1014-1024, Mar. 2004.
- [58] F. Congedo, G. Monti, L. Tarricone, M. Cannarile, "Broadband Bowtie Antenna for RF Energy Scavenging Applications," in *Proc. IEEE 5th Euro. Conf. on Antennas and Propagation*, Berlin, Germany, Mar. 2009, pp. 1-3.
- [59] W. S. Yeoh, "Wireless Power Transmission (WPT) Application at 2.45GHz in Common Network," Ph.D. dissertation, School of Elect. And Comp. Eng., RMIT Univ., March 2010.
- [60] G. Vera, A. Georgiadis, A. Collado, and S. Via, "Design of a 2.45 GHz rectenna for electromagnetic (EM) energy scavenging," in *Proc. IEEE Radio Wireless Symp.*, 2010, pp. 61–64.
- [61] Rivière S, Alicalapa F, Douyère A and Lan Sun Luk, "A compact rectenna device at low power level," *Progress In Electromagnetic Research C* 16 137-146.
- [62] D. H. Chuc and B. G. Duong, "Design, simulation and fabrication of rectenna circuit at S-Band for microwave power transmission," *VNU J. Sci., Math.-Phys.*, vol. 30, no. 3, pp. 24–30, 2014.

- [63] F.-J. Huang, C.-M. Lee, C.-L. Chang, L.-K. Chen, T.-C. Yo, and C.-H. Luo, "Rectenna application of miniaturized implantable antenna design for triple-band biotelemetry communication," *IEEE Trans. Antennas Propag.*, vol. 59, no. 7, pp. 2646–2653, Jul. 2011
- [64] Tan, Lee Meng Mark, "Efficient rectenna Design for Wireless Power Transmission for MAV Applications," Master Thesis, 2005.
- [65] G. Indumathi and K. Karthika, "Rectenna Design for RF Energy Harvesting in Wireless Sensor Networks," *IEEE International Conference on Electrical, Computer and Communication Technologies (ICECCT)*, pp.1-4, Mar 2015.
- [66] Z. Popovic, E. A. Falkenstein, D. Costinett, and R. Zane, "Low-power far-field wireless powering for wireless sensors," *Proc. IEEE*, vol. 101, no. 6, pp. 1397–1409, Jun. 2013.
- [67] E. M. Ali, N. Z. Yahaya, N. Perumal and M. A. Zakariya, "Design and development of harvester RECTENNA at GSM band for battery charging applications", *Journal of Engineering and Applied Sciences*, 10(21): 10206-10212, 2015
- [68] J. Ramsay, "Highlights of antenna history," *IEEE Antennas Propag. Society Newslett.*, vol. 23, pp. 7–20, Dec. 1981.
- [69] T. W. Barton, J. Gordonson, and D. J. Perreault, "Transmission line resistance compression networks and applications to wireless power transfer," *IEEE J. Emerg. Sel. Topics Power Electron.* Vol.1, Issue 1, pp. 252 – 260, 21 April 2014.
- [70] P. Godoy, D. Perreault, and J. Dawson, "Outphasing energy recovery amplifier with resistance compression for improved efficiency," *IEEE Trans. Microw. Theory Techn.*, vol. 57, no. 12, pp. 2895–2906, Dec. 2009.
- [71] W. Nitz *et al.*, "A new family of resonant rectifier circuits for high frequency DC-DC converter applications," in *Proc. 3rd Annu. IEEE APEC Expo*, Feb. 1988, pp. 12–22.
- [72] S. Keyrouz, H. Visser, and A. Tijhuis, "Rectifier analysis for radio frequency energy harvesting and power transport," in *Proc. 42nd IEEE Eur. Microwave Conf.*, Oct./Nov. 2012, pp. 428–431.
- [73] Y. Han, O. Leitermann, D. A. Jackson, J. M. Rivas, and D. J. Perreault, "Resistance compression networks for radio-frequency power conversion," *IEEE Trans. Power Electron.*, vol. 22, no. 1, pp. 41–53, Jan. 2007.
- [74] H. Visser, "Aspects of far-field RF energy transport," in *Proc. 42nd IEEE Eur. Microwave Conf.*, Oct./Nov. 2012, pp. 317–320.

- [75] J. Santiago-Gonzalez, K. Afridi, and D. Perreault, "Design of resistive input class-E resonant rectifiers for variable-power operation," in *Proc. IEEE 14th Workshop Control and Modeling Power Electron.*, Jun. 2013, pp. 1–6.
- [76] J. McSpadden, T. Yoo, and K. Chang, "Theoretical and experimental investigation of a rectenna element for microwave power transmission," *IEEE Trans. Microw. Theory Techn.*, vol. 40, no. 12, pp. 2359–2366, Dec. 1992.
- [77] G. A. Vera, A. Georgiadis, A. Collado, and S. Via, "Design of a 2.45 GHz rectenna for electromagnetic (EM) energy scavenging," in *Proc. IEEE RWS*, Jan. 2010, pp. 61–64.
- [78] M. D. Prete, A. Costanzo, D. Masottii, and A. Romani, "An alternative rectenna design approach for wirelessly powered energy autonomous systems," in *IEEE MTT-S IMS Dig.*, Jun. 2013, pp. 1–4.
- [79] Y. Huang, N. Shinohara, and T. Mitani, "A study on low power rectenna using DC-DC converter to track maximum power point," in *Proc. APMC*, Nov. 2013, pp. 83–85.
- [80] M. Dini *et al.*, "A fully-autonomous integrated RF energy harvesting system for wearable applications," in *Proc. Eur. Microwave Conf.*, Oct. 2013, pp. 987–990.
- [81] Roger O4350B:<https://www.rogerscorp.com/acs/products/55/RO4350B-Laminates.aspx> [Accessed: July-2017].
- [82] L. M. M. Tan, "Efficient rectenna design for wireless power transmission for MAV applications," M. Sci. thesis, Naval Postgraduate School, Monterey, California, Dec. 2005
- [83] William C. Brown, "The History of Power Transmission by Radio Waves," *IEEE Transactions of Microwave Theory and Techniques*, Vol MTT-32. No. 9, September 1984.
- [84] James O. McSpadden, Taewhan Yoo, and Kai Chang, "Theoretical and Experimental Investigation of a Rectenna Element for Microwave Power Transmission," *IEEE Transactions on Microwave Theory and Techniques*, Vol. 40, No. 12, Dec 1992.
- [85] D. Pozar, "Microwave Engineering," Third Edition, *John Wiley & Sons, Inc.*, New Jersey, Ch. 13, pp. 98-106, 2005.
- [86] V. Salas, E. Olias, A. Barrado, A. Lazaro, "Review of the maximum power point tracking algorithms for stand-alone photovoltaic systems", *Solar Energy Materials and Solar Cells*, vol.90, no.11, pp.1555-1578, 2006
- [87] E. Koutroulis and K. Kalaitzakis, "Design of a maximum power tracking system for wind-energy-conversion applications", *IEEE Transactions on Industrial Electronics*, vol.53, issue.2, pp.486-494, 2006.

- [88] M. S. Ngan, C. W. Tan, "A study of maximum power point tracking algorithms for stand-alone Photovoltaic Systems," in *Proc. of IEEE Applied Power Electronics Colloquium*, pp.22-27, 2011.
- [89] D. Lafferty, Coupling network for improving conversion efficiency of photovoltaic power source, US4, 873,480, 1989.
- [90] P. Chetty, Maximum power transfer system for a solar cell array, US4,604,567, 1986.
- [91] M.A.S. Masoum, et al., Optimal power point tracking of photovoltaic system under all operating conditions, in: 17th Congress of the World Energy Council, Houston, TX, 1998.
- [92] M.A.S. Masoum, *et al*, "Design, construction and testing of a voltage-based maximum power point tracker (VMPPT) for small satellite power supply," in: *13th Annual AIAA/USU Conference, Small Satellite*, 1999.
- [93] J.J. Schoeman, J.D. van Wyk," A simplified maximal power controller for terrestrial photovoltaic panel arrays," *IEEE Power Electronics Specialists Conference*. New York, NY, 1982, pp. 361–367.
- [94] S.M. Alghuwainem, "Matching of a dc motor to a photovoltaic generator using a step-up converter with a current-locked loop," *IEEE Trans. Energy Conversion* 9 (1994) 192–198.
- [95] T. Noguchi, et al., "Short-current pulse-based adaptive maximum power point tracking for a photovoltaic power generation system," *Elect. Eng. Japan* 139 (1) (2002) 65–72.
- [96] H.D. Maheshappa, J. Nagaraju, M.V. Murthy, "An improved maximum power point tracker using a step-up converter with current locked loop," *Renew. Energy* 13 (2) (1998) 195–201.
- [97] Ch. Hua, Ch. Shen, "Comparative study of peak power tracking techniques for solar storage system," in: *IEEE Applied Power Electronics Conference and Exposition (APEC'98)*, vol. 2, 1998, pp. 679–685.
- [98] J.H. David, Power conditioning system, US3,384,806, 1968
- [99] L.T.W. Bavaro, Power regulation utilizing only battery current monitoring, Patent, US4, 794,272, 1988.
- [100] Z. Salameh, D. Taylor, "Step-up maximum power point tracker for photovoltaic arrays," *Solar Energy* 44 (1) (1990) 57–61.
- [101] W. Denizinger," Electrical power subsystem of global star," in: *Proceedings of the European Space Conference*, 1995, pp. 171–174.

- [102] W.J.A. Teulings, J.C. Marpinard, A. Capel, "A maximum power point tracker for a regulated power bus," in: *Proceedings of the European Space Conference*, 1993.
- [103] Y. Kim, H. Jo, D. Kim, "A new peak power tracker for cost-effective photovoltaic power systems," *IEEE Proc. Energy Conversion Eng. Conf. IECEC 96* Vol. 3 (1996) 1673–1678.
- [104] Ch. Hua, J. Lin, Ch. Shen, "Implementation of a DSP-controlled PV system with peak power tracking," *IEEE Trans. Ind. Electron.* Vol.45 (1) (1998) 99–107
- [105] H. Al-Atrash, I. Batarseh, K. Rustom, "Statistical modeling of DSP-based hill-climbing MPPT algorithms in noisy environments," *Applied Power Electronics Conference and Exposition, 2005. APEC 2005, Twentieth Annual IEEE*, vol. 3, 6–10 March 2005, pp. 1773–1777.
- [106] K.H. Hussein, I. Muta, T. Hoshino, M. Osakada, "Maximum photovoltaic power tracking: an algorithm for rapidly changing atmospheric conditions," *IEEE Proc. Generation Transmission Distrib.* 142 (1) (1995) 59–64.
- [107] K. Khouzam & L. Khouzam, "Optimum matching of direct-coupled electromechanical loads to a photovoltaic generator", *IEEE Transaction on Energy Conversion*, vol.8, issue.3, pp.343-349, 1993.
- [108] R. W. Erickson, D. Maksimovic, *Fundamentals of Power Electronics*, 2nd ed., Springer Science + Business Media, Inc., New York, NY, 2001 , pp. 637-663.
- [109] Linear Technology LTC6906: <http://cds.linear.com/docs/en/datasheet/6906fc.pdf>
- [110] M. S. H. Al Salameh, Majdi. M. Ababneh, "Selecting Printed Circuit Board Parameters Using Swarm Intelligence to Minimize Crosstalk between Adjacent Tracks", In the *International Journal of Numerical Modelling: Electronic Networks, Devices and Fields*, June 2012
- [111] R. C. Eberhart and Y. Shi," Particle swarm optimization: developments, applications and resources," *Proc. 2001 Congr. Evolutionary Computation*, 2001
- [112] Kennedy J and Eberhart R, " Particle swarm optimization," *IEEE Int. Conf. on Neural Networks*, NJ, USA, 1995; 4:1942-1948.
- [113] Robinson J and Rahmat Samii Y," Particle swarm optimization in electromagnetic," *IEEE Transactions on Antenna and Propagations*, 2004; 52(2): 397 – 407.
- [114] Majdi Ababneh, ' Printed circuit board (PCB) design with minimum cross-talk between adjacent traces using swarm intelligence,' Master thesis, 2012

- [115] Parsopoulos and Vrahattmn, "On the computation of all global minimizes through particle swarm optimization," *IEEE Transactions on Evolutionary Computation*, 2004, 8(3): 211-224.
- [116] El-Abd M and Kamel M, "Swarm Intelligence: A cooperative particle swarm optimizer with migration of heterogeneous probabilistic models," Springer, New York 2010; 57-89.
- [117] Khodier M M, Christodoulou CG,"Linear array geometry synthesis with minimum side lobe level and null control using particle swarm optimization," *In: IEEE Trans. on Antenna and Propagations* 2005; 53(8): 2674 – 2679.
- [118] Premalatha K, Natarajan A," Hybrid PSO and GA for Global Maximization," *Int. J. Open Problems Compt. Math. International Center for Scientific Research and Studies* December 2009; 2(4).
- [119] Moradi A M,Darlane AB," Particle swarm optimization: application to reservoir operation problems," *In: IEEE Int. Advance Computing Conf. (IACC)*. Patiala.2009; 1048 – 1051.
- [120] Jaco F. Schutte. The Particle Swarm Optimization Algorithm. EGM 6365 - Structural Optimization Fall 2005.
- [121] Wang L, Cui Z, Zeng J,"Particle swarm optimization with group decision making," *In: 9th Int. Conf. on Hybrid Intelligent Systems*. Shenyang. 2009; 388-393.
- [122] El-Abd M, Kamel M, Swarm Intelligence. In: A cooperative particle swarm optimizer with migration of heterogeneous probabilistic models, Springer, New York 2010; 57-89.
- [123] Coelho LDS, Alotto P, "Global optimization of electromagnetic devices using an exponential quantum-behaved particle swarm optimizer," *In: IEEE Trans. on Magnetics* 2008; 44(6): 1074–1077.
- [124] EnFilm™ - rechargeable solid state lithium thin film battery, STMicroelectronics <http://www.st.com/en/power-management/efl1k0af39.html>
- [125] Majdi M. Ababneh, Samuel Perez, and Sylvia Thomas, "Design of a SiC Implantable Rectenna for Wireless In-Vivo Biomedical Devices," *The 8th IEEE Annual Ubiquitous Computing, Electronics & Mobile Communication Conference*, October 2017
- [126] B. Zhang, X. Zhao, C. Yu, K. Huang, C. Liu, "A Power Enhanced High Efficiency 2.45 GHz Rectifier Based on Diode Array", *Journal of Electromagnetic Waves and Applications*, vol. 25, pp. 765, 2011, ISSN 0920-5071

- [127] N. Femia, G. Petrone, G. Spagnulo, M. Viteli, "Optimization of perturb and observe maximum power point tracking method," *IEEE Transactions on Power Electronics*, Jul. 2005, vol. 20, no. 4, pp. 963-973.
- [128] K. H. Hussein, I. Muta, T. Hshino, and M. Osakada, "Maximum photovoltaic power tracking: an algorithm for rapidly changing atmospheric conditions," *Proc. Inst. Elect. Eng.*, vol. 142, no. 1, pp. 59–64, Jan. 1995.
- [129] K. K. Tse, M. T. Ho, H. S.-H. Chung, and S. Y. Hui, "A novel maximum power point tracker for PV panels using switching frequency modulation," *IEEE Trans. Power Electron.*, vol. 17, no. 6, pp. 980–989, Nov. 2002.
- [130] D. P. Hohm and M. E. Ropp, "Comparative study of maximum power point tracking algorithms," in *Proc. 28th IEEE Photovoltaic Specialists Conf.*, Sep. 2000, pp. 1699–1702.

APPENDICES

Appendix A: Data of Figures 4.6, 4.7, 4.11, and 4.12

Table A.1: Power Conversion Efficiency of Enhanced Power Management Circuit for Low Input Power Range Using MiNT

Power input (μW)	Power output (μW)	Power loss (μW)	Simulated converter efficiency %	Measured converter efficiency %
50	18.04	31.96	40.8	36.08
75	36	39	52	48
100	56.68	43.32	64.8	56.68
125	81.68	43.75	70.5	65
150	105.162	44.83	74.8	70.108
175	129.5	45.5	77.5	74
200	149.4	50.6	79.7	74.7
225	175.05	49.95	81	77.8
250	197	53	82.8	78.8
275	219.725	55.275	83.8	79.9
300	235.2	64.8	84.76	78.4
325	256.946	68.05	85.52	79.06
350	283.78	66.22	86.35	81.08
375	307.87	67.125	86.84	82.1
400	328.429	71.57	87.36	82.107
425	348.963	76.06	87.8	82.109
450	374.512	75.48	88.25	83.225
475	401.37	73.62	88.9	84.5
500	424.65	75.35	89.3	84.93

Table A.2: Power Conversion Efficiency of Enhanced Power Management Circuit for High Input Power Range Using MiNT

Power input (mW)	Power output (mW)	Power loss (mW)	Simulated converter efficiency %	Measured converter efficiency %
1	0.867	0.1330	92.5	86.7
2	1.7388	0.2612	93.6	86.942
3	2.62	0.372	94.8	87.6
4	3.488	0.512	95	87.2
5	4.35	0.65	95.1	87
6	5.25	0.75	95.1	87.5
7	6.139	0.861	95.2	87.7
8	7	0.992	95.2	87.6
9	7.902	1.098	95.3	87.8
10	8.78	1.22	95.4	87.8
11	9.702	1.298	95.5	88.2
12	10.63	1.368	95.6	88.6
13	11.544	1.456	95.6	88.8
14	12.54	1.45	95.6	89.6
15	13.542	1.4577	95.7	90.282

Table A.3: Power Conversion Efficiency of Enhanced Power Management Circuit for Low Input Power Range Using RF Rectenna

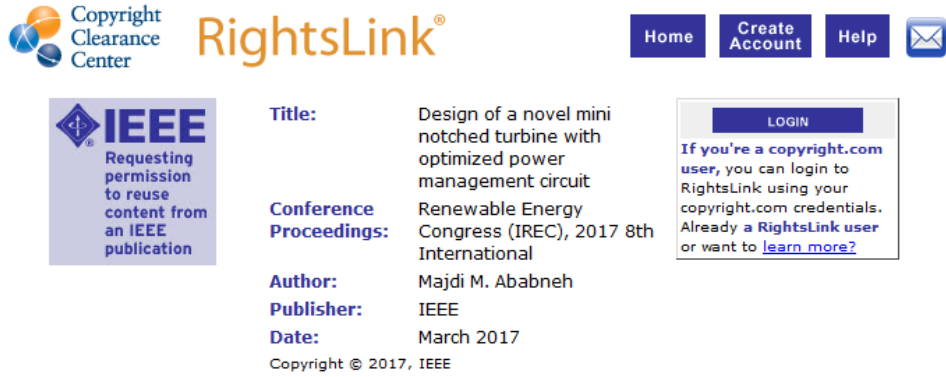
Power input (μW)	Power output (μW)	Power loss (μW)	Simulated converter efficiency%	Measured converter efficiency %
200	148	52	77.5	74
225	170.1	54.9	79.7	75.6
250	194.5	55.5	81	77.8
275	216.7	58.3	82.8	78.8
300	238.5	61.5	83.8	79.5
325	259.35	65.65	84.8	79.8
350	281.7	68.21	85.8	80.5
375	304.05	90.95	86.3	81.08
400	328.4	71.6	86.8	82.1
425	350.67	74.326	87.36	82.5
450	372.64	77.36	87.8	82.8
475	395	79.68	88	83.2
500	417.5	82.5	88.25	83.5
550	462	88	88.4	84
600	505.2	94.8	88.9	84.2
650	549.25	100.75	89	84.5
700	592.9	107.1	89.3	84.7
750	636.7	113.2	89.6	84.9

Table A.4: Power Conversion Efficiency of Enhanced Power Management Circuit for High Input Power Range Using RF Rectenna

Power input (mW)	Power output (mW)	Power loss (mW)	Simulated converter efficiency %	Measured converter efficiency %
1	0.85	0.15	92.5	85
2	1.704	0.296	93.6	85.2
3	2.565	0.435	94.8	85.5
4	3.48	0.52	95	87
5	4.25	0.75	95.1	85
6	5.106	0.894	95.1	85.1
7	5.964	1.036	95.2	85.2
8	7.008	0.992	95.2	87.6
9	7.902	1.098	95.3	87.8
10	8.78	1.22	95.4	87.8
11	9.68	1.32	95.5	88
12	10.63	1.368	95.6	88.6
13	11.18	1.82	95.6	86
14	12.544	1.456	95.6	89.6
15	13.53	1.47	95.7	90.2
16	14.432	1.568	95.7	90.2
17	15.35	1.649	95.8	90.3
18	16.236	1.7640	95.8	90.2
19	17.19	1.805	95.8	90.5
20	18.16	1.84	95.8	90.8

Appendix B: Copyright Notices

The following notice is for the material in Chapter 2, 3, and 4.



The screenshot shows the Copyright Clearance Center RightsLink interface. At the top left is the Copyright Clearance Center logo. To its right is the RightsLink logo. Further right are navigation buttons for Home, Create Account, Help, and an email icon. Below the logo is a blue box with the IEEE logo and the text "Requesting permission to reuse content from an IEEE publication". To the right of this box is a list of document details: Title: Design of a novel mini notched turbine with optimized power management circuit; Conference Proceedings: Renewable Energy Congress (IREC), 2017 8th International; Author: Majdi M. Ababneh; Publisher: IEEE; Date: March 2017; Copyright © 2017, IEEE. To the right of the details is a LOGIN button and a text box that says "If you're a copyright.com user, you can login to RightsLink using your copyright.com credentials. Already a RightsLink user or want to learn more?".

Thesis / Dissertation Reuse

The IEEE does not require individuals working on a thesis to obtain a formal reuse license, however, you may print out this statement to be used as a permission grant:

Requirements to be followed when using any portion (e.g., figure, graph, table, or textual material) of an IEEE copyrighted paper in a thesis:

- 1) In the case of textual material (e.g., using short quotes or referring to the work within these papers) users must give full credit to the original source (author, paper, publication) followed by the IEEE copyright line © 2011 IEEE.
- 2) In the case of illustrations or tabular material, we require that the copyright line © [Year of original publication] IEEE appear prominently with each reprinted figure and/or table.
- 3) If a substantial portion of the original paper is to be used, and if you are not the senior author, also obtain the senior author's approval.

Requirements to be followed when using an entire IEEE copyrighted paper in a thesis:

- 1) The following IEEE copyright/ credit notice should be placed prominently in the references: © [year of original publication] IEEE. Reprinted, with permission, from [author names, paper title, IEEE publication title, and month/year of publication]
- 2) Only the accepted version of an IEEE copyrighted paper can be used when posting the paper or your thesis on-line.
- 3) In placing the thesis on the author's university website, please display the following message in a prominent place on the website: In reference to IEEE copyrighted material which is used with permission in this thesis, the IEEE does not endorse any of [university/educational entity's name goes here]'s products or services. Internal or personal use of this material is permitted. If interested in reprinting/republishing IEEE copyrighted material for advertising or promotional purposes or for creating new collective works for resale or redistribution, please go to http://www.ieee.org/publications_standards/publications/rights/rights_link.html to learn how to obtain a License from RightsLink.

If applicable, University Microfilms and/or ProQuest Library, or the Archives of Canada may supply single copies of the dissertation.

BACK

CLOSE WINDOW

Copyright © 2018 Copyright Clearance Center, Inc. All Rights Reserved. [Privacy statement](#). [Terms and Conditions](#).

Comments? We would like to hear from you. E-mail us at customercare@copyright.com

The following notice is for the material in Chapter 2, 3, and 4.



RightsLink®

Home

Create Account

Help



Title: Optimized mini notched turbine energy harvesting using resistor emulation approach and Particle Swarm Optimization

Conference Proceedings: SoutheastCon, 2017

Author: Majdi M. Ababneh

Publisher: IEEE

Date: March 2017

Copyright © 2017, IEEE

LOGIN

If you're a copyright.com user, you can login to RightsLink using your copyright.com credentials. Already a RightsLink user or want to [learn more?](#)

Thesis / Dissertation Reuse

The IEEE does not require individuals working on a thesis to obtain a formal reuse license, however, you may print out this statement to be used as a permission grant:

Requirements to be followed when using any portion (e.g., figure, graph, table, or textual material) of an IEEE copyrighted paper in a thesis:

- 1) In the case of textual material (e.g., using short quotes or referring to the work within these papers) users must give full credit to the original source (author, paper, publication) followed by the IEEE copyright line © 2011 IEEE.
- 2) In the case of illustrations or tabular material, we require that the copyright line © [Year of original publication] IEEE appear prominently with each reprinted figure and/or table.
- 3) If a substantial portion of the original paper is to be used, and if you are not the senior author, also obtain the senior author's approval.

Requirements to be followed when using an entire IEEE copyrighted paper in a thesis:

- 1) The following IEEE copyright/ credit notice should be placed prominently in the references: © [year of original publication] IEEE. Reprinted, with permission, from [author names, paper title, IEEE publication title, and month/year of publication]
- 2) Only the accepted version of an IEEE copyrighted paper can be used when posting the paper or your thesis on-line.
- 3) In placing the thesis on the author's university website, please display the following message in a prominent place on the website: In reference to IEEE copyrighted material which is used with permission in this thesis, the IEEE does not endorse any of [university/educational entity's name goes here]'s products or services. Internal or personal use of this material is permitted. If interested in reprinting/republishing IEEE copyrighted material for advertising or promotional purposes or for creating new collective works for resale or redistribution, please go to http://www.ieee.org/publications_standards/publications/rights/rights_link.html to learn how to obtain a License from RightsLink.

If applicable, University Microfilms and/or ProQuest Library, or the Archives of Canada may supply single copies of the dissertation.

BACK

CLOSE WINDOW

Copyright © 2018 [Copyright Clearance Center, Inc.](#) All Rights Reserved. [Privacy statement](#). [Terms and Conditions](#).

Comments? We would like to hear from you. E-mail us at customercare@copyright.com

The following notice is for the material in Chapter 2, 3, and 4.



RightsLink®

Home

Create Account

Help



Title: Optimized power management circuit for RF energy harvesting system
Conference Proceedings: Wireless and Microwave Technology Conference (WAMICON), 2017 IEEE 18th
Author: Majdi M. Ababneh
Publisher: IEEE
Date: April 2017
Copyright © 2017, IEEE

LOGIN

If you're a copyright.com user, you can login to RightsLink using your copyright.com credentials. Already a RightsLink user or want to [learn more?](#)

Thesis / Dissertation Reuse

The IEEE does not require individuals working on a thesis to obtain a formal reuse license, however, you may print out this statement to be used as a permission grant:

Requirements to be followed when using any portion (e.g., figure, graph, table, or textual material) of an IEEE copyrighted paper in a thesis:

- 1) In the case of textual material (e.g., using short quotes or referring to the work within these papers) users must give full credit to the original source (author, paper, publication) followed by the IEEE copyright line © 2011 IEEE.
- 2) In the case of illustrations or tabular material, we require that the copyright line © [Year of original publication] IEEE appear prominently with each reprinted figure and/or table.
- 3) If a substantial portion of the original paper is to be used, and if you are not the senior author, also obtain the senior author's approval.

Requirements to be followed when using an entire IEEE copyrighted paper in a thesis:

- 1) The following IEEE copyright/ credit notice should be placed prominently in the references: © [year of original publication] IEEE. Reprinted, with permission, from [author names, paper title, IEEE publication title, and month/year of publication]
- 2) Only the accepted version of an IEEE copyrighted paper can be used when posting the paper or your thesis on-line.
- 3) In placing the thesis on the author's university website, please display the following message in a prominent place on the website: In reference to IEEE copyrighted material which is used with permission in this thesis, the IEEE does not endorse any of [university/educational entity's name goes here]'s products or services. Internal or personal use of this material is permitted. If interested in reprinting/republishing IEEE copyrighted material for advertising or promotional purposes or for creating new collective works for resale or redistribution, please go to http://www.ieee.org/publications_standards/publications/rights/rights_link.html to learn how to obtain a License from RightsLink.

If applicable, University Microfilms and/or ProQuest Library, or the Archives of Canada may supply single copies of the dissertation.

BACK

CLOSE WINDOW

Copyright © 2018 Copyright Clearance Center, Inc. All Rights Reserved. [Privacy statement](#). [Terms and Conditions](#).

Comments? We would like to hear from you. E-mail us at customercare@copyright.com

The following notice is for the material in Chapter 2, 3, and 4.



RightsLink®

Home

Create Account

Help



Title: Design of a SiC implantable rectenna for wireless in-vivo biomedical devices
Conference Proceedings: Ubiquitous Computing, Electronics and Mobile Communication Conference (UEMCON), 2017 IEEE 8th Annual
Author: Majdi M. Ababneh
Publisher: IEEE
Date: Oct. 2017
Copyright © 2017, IEEE

LOGIN

If you're a [copyright.com user](#), you can login to RightsLink using your copyright.com credentials. Already a [RightsLink user](#) or want to [learn more?](#)

Thesis / Dissertation Reuse

The IEEE does not require individuals working on a thesis to obtain a formal reuse license, however, you may print out this statement to be used as a permission grant:

Requirements to be followed when using any portion (e.g., figure, graph, table, or textual material) of an IEEE copyrighted paper in a thesis:

- 1) In the case of textual material (e.g., using short quotes or referring to the work within these papers) users must give full credit to the original source (author, paper, publication) followed by the IEEE copyright line © 2011 IEEE.
- 2) In the case of illustrations or tabular material, we require that the copyright line © [Year of original publication] IEEE appear prominently with each reprinted figure and/or table.
- 3) If a substantial portion of the original paper is to be used, and if you are not the senior author, also obtain the senior author's approval.

Requirements to be followed when using an entire IEEE copyrighted paper in a thesis:

- 1) The following IEEE copyright/ credit notice should be placed prominently in the references: © [year of original publication] IEEE. Reprinted, with permission, from [author names, paper title, IEEE publication title, and month/year of publication]
- 2) Only the accepted version of an IEEE copyrighted paper can be used when posting the paper or your thesis on-line.
- 3) In placing the thesis on the author's university website, please display the following message in a prominent place on the website: In reference to IEEE copyrighted material which is used with permission in this thesis, the IEEE does not endorse any of [university/educational entity's name goes here]'s products or services. Internal or personal use of this material is permitted. If interested in reprinting/republishing IEEE copyrighted material for advertising or promotional purposes or for creating new collective works for resale or redistribution, please go to http://www.ieee.org/publications_standards/publications/rights/rights_link.html to learn how to obtain a License from RightsLink.

If applicable, University Microfilms and/or ProQuest Library, or the Archives of Canada may supply single copies of the dissertation.

BACK

CLOSE WINDOW

Copyright © 2018 [Copyright Clearance Center, Inc.](#) All Rights Reserved. [Privacy statement.](#) [Terms and Conditions.](#)

Comments? We would like to hear from you. E-mail us at customer@copyright.com

Appendix C: Glossary of Terms

RF	Radio Frequency
PSO	Particle Swarm Optimization
MiNT	Mini Notched Turbine
MPPT	Maximum Power Point Tracking
V_n	Nozzle velocity
P_{Flow}	Available Power in Fluid
T_T	Total Torque,
w	Angular Velocity,
U_1	Tangential Velocity on Rotor
ρ	Fluid Density in kg/m^3
η_{Hy}	Hydromechanical Efficiency of MiNT
P_R	Mechanical Rotor Power
P_E	Electrical Power Output of MiNT
I_D	Diode Current
I_S	Reverse Saturation Current
K	Boltzmann Constant
T	Absolute Temperature
N	Ideality Factor
SiC	Silicon Carbide
S_{11}	Return Loss
P_{density}	Power Density
P_1	Output Power of Rectenna

A_e	Effective Area for Patch Antenna
λ	Wavelength
G	Antenna Gain
L_p	Actual Length of Patch Antenna
L_{eff}	Effective Length of Patch Antenna
ΔL	Extended patch length,
c	Speed of Light,
f	Operating Frequency,
ϵ_e	Effective Dielectric Constant,
h_p	Height of Patch Antenna
ϵ_r	Dielectric Constant
$\tan\delta$	Tangent Loss
C_p	Diode's Parasitic Capacitance
L_p	Diode's Parasitic Inductance
R_s	Series Resistance
R_j	Junction Resistance
C_j	Junction Capacitance
P&O	Perturbation and Observe Technique
D	Duty Cycle
Q_g	Gate Capacitance of MOSFET
C_{oss}	Output Capacitance of MOSFET
R_{ESR}	Equivalent Series Resistance of Inductor
v'_{id}	Current Velocity of Particle i in d^{th} Dimension

v_{id}^{t-1}	Previous Velocity
l_{id}^{t-1}	Previous Position
c_1, c_2	User-Defined Constants
p_{id}^t	Current pbest,
g_d^t	Current Global Solution,
r_{d1}^t, r_{d2}^t	Random Numbers in the range of [0, 1]
l_{id}^t	New Position
l_{id}^{t-1}	Previous Position
Δt	Time Step

ABOUT THE AUTHOR

Majdi M. Ababneh received the B.Sc. and the M.Sc. degree from Jordan University of Science and Technology (JUST), Jordan, in 2009 and 2012, respectively; all in electrical engineering. In 2013, he joined the advanced materials bio & integration research laboratory (AMBIR) at the University of South Florida, Tampa, FL, as a graduate research assistant. His current research is focused on renewable energy harvesting and their applications, power electronics, RF circuit design, integration of bio-applications in nano-scaled technology, power management circuit design, and MPPT.